Journal of Academic Research and Advances

Contents

Deep Learning-Based Object Tracking for Augmented Reality: A System-Level Survey of Methods, Constraints, and Challenges

Mou Duoduo[1*]

[1] Faculty of Computing, Universiti Teknologi Malaysia, Skudai, Johor 81310, Malaysia
* Correspondence: mouduoduo@graduate.utm.my

https://doi.org/10.53104/j.acad.res.adv.2026.03001

Abstract: The immersiveness and usability of augmented reality (AR) systems rely on accurate, temporally stable, and computationally efficient object tracking. Recent advances in deep learning have reshaped visual tracking and enabled increasingly complex AR applications on mobile and edge platforms. As AR progresses toward large-scale consumer and industrial deployment, tracking has become a system-critical perception module that directly affects visual stability, interaction latency, and user trust. This survey reviews deep learning based object tracking for AR from 2018 to 2025, focusing on algorithmic paradigms and system-level constraints. We analyze AR-specific requirements such as tight latency budgets, limited energy, long-term operation, and perceptual stability, and examine four representative paradigms (Siamese networks, deep discriminative correlation filters, Transformer based models, and long-term frameworks) with their design rationales and deployment challenges. We further discuss lightweight architectures, state-space temporal models, and diffusion-based approaches, along with integration strategies involving efficiency optimization, hardware-aware design, 6-DoF pose tracking, SLAM coupling, neural scene representations, and multimodal fusion. Representative datasets and evaluation protocols are analyzed from an AR deployment viewpoint, and open challenges and future research directions are identified. We argue that AR-oriented tracking constitutes a distinct research domain where algorithmic accuracy, perceptual stability, and system efficiency must be jointly optimized to support trustworthy and immersive next-generation AR experiences.

Keywords: augmented reality; object tracking; deep learning; transformer; lightweight models; multimodal fusion; 6-dof pose estimation

Received: 30 January 2026

Revised: 12 March 2026

Accepted: 16 March 2026

Published: 23 April 2026

Citation: Mou, D. (2026) 'Deep Learning-Based Object Tracking for Augmented Reality: A System-Level Survey of Methods, Constraints, and Challenges', *Journal of Academic Research and Advances*, 2(1), pp. 1-14.

Copyright: © 2026 by the authors. This article is an open access article distributed under the terms and conditions of the Creative Commons Attribution (CC BY) license (https://creativecommons.org/licenses/by/4.0/).

OPEN ACCESS

1. Introduction

Augmented reality (AR) enhances human perception by superimposing digital content onto the physical world, enabling transformative applications in human–computer interaction, industrial inspection and maintenance, medical intervention, education, and consumer entertainment. A compelling AR experience fundamentally relies on the seamless spatial alignment between virtual content and the physical environment, which in turn requires continuous, accurate, and temporally stable perception. Among the various perception components in an AR pipeline, object tracking plays a central role by continuously estimating the position, scale, and, in many cases, the full six-degree-of-freedom (6-DoF) pose of target objects across time (Danelljan et al., 2020).

Accurate tracking ensures that virtual objects remain correctly anchored to their physical counterparts during user interaction, while even minor localization jitter or drift can immediately degrade perceptual quality and induce discomfort. With the rapid evolution of mobile computing platforms such as smartphones, tablets, and head mounted AR displays and major advances in deep learning, object tracking has progressed from handcrafted feature based methods to data driven approaches with substantially improved robustness and accuracy (Dai et al., 2020). Modern trackers exhibit strong resilience to challenging factors such as illumination variation, motion blur, occlusion, background clutter, and nonrigid deformation.

Accordingly, this survey aims to reposition object tracking within the broader context of AR system design. Rather than treating tracking as an isolated vision problem, we adopt a system-oriented perspective that explicitly accounts for perceptual stability, latency, energy efficiency, and long-term deployment constraints. By synthesizing recent advances across algorithms, system optimization, and evaluation methodologies, this survey seeks to provide both a structured reference for researchers and a practical guide for practitioners developing next-generation AR systems.

1.1 Contributions of this Survey

This survey differs from existing reviews in several important aspects. First, we explicitly frame AR-oriented object tracking as a system-level perception problem rather than an isolated vision task. Second, we provide a unified analysis of major deep learning tracking paradigms through the lens of AR-specific constraints, systematically comparing their algorithmic characteristics, temporal stability, and deployment efficiency on mobile and edge platforms. Third, we emphasize recent developments particularly relevant to AR deployment, including lightweight Transformer architectures, state-space temporal modeling, multimodal perception fusion, and tight integration with SLAM and scene understanding. Finally, we identify open challenges and future research directions that must be addressed to bridge the gap between benchmark-level tracking performance and reliable, long-term AR deployment.

2. Object Tracking in AR: Definitions, Challenges, and Evaluation

Object tracking in augmented reality (AR) differs fundamentally from generic visual tracking tasks studied in traditional computer vision. Rather than serving as an isolated perception module, tracking in AR operates within a tightly coupled, closed-loop system that integrates sensing, rendering, interaction, and user perception. As a result, the design objectives, evaluation criteria, and failure modes of AR-oriented tracking are significantly reshaped by system-level and perceptual constraints. This section formalizes the task definition of object tracking in AR systems, analyzes the unique challenges imposed by AR deployment scenarios, and reviews evaluation criteria that more accurately reflect real-world AR performance.

2.1 Task Definition and System-Level Integration

In AR systems, object tracking aims to continuously estimate the spatial state of a target object across time, typically represented as a two-dimensional bounding box in image coordinates or a full six-degree-of-freedom (6-DoF) pose in camera or world coordinates (Labbé et al., 2020). Unlike offline tracking benchmarks, AR tracking outputs are consumed immediately by downstream modules, including rendering engines, physics simulators, and interaction logic, forming a closed perception-action loop.

A typical AR tracking pipeline consists of several tightly coupled stages. Initialization may be triggered by automatic object detection, user interaction, or prior scene knowledge. Once initialized, the tracker extracts visual features to model the target's appearance and estimates motion using frame-to-frame correspondence, temporal filtering, or inertial priors (Hodan et al., 2020). Online adaptation mechanisms update the appearance model to accommodate gradual changes, while failure recovery strategies handle occlusion, out-of-view events, or tracking loss.

Crucially, these stages are not independent. Tracking estimates influence rendering and interaction, while rendering feedback and user motion affect subsequent observations. This bidirectional coupling means that tracking errors propagate directly to perceptual artifacts, such as visual jitter, spatial drift, or delayed response, which are immediately noticeable to users (Chen et al., 2021). Consequently, AR tracking must be designed and evaluated as a system-level capability rather than a standalone algorithm.

2.2 Unique Challenges in AR Scenarios

AR applications impose stringent real time constraints that exceed generic tracking benchmarks, requiring 60–90 Hz tracking for visual comfort and end to end latency below 20 ms (Wang et al., 2021). Mobile, battery powered platforms further impose tight energy budgets, shifting the design objective from pure accuracy to a balance among accuracy, latency, and energy efficiency. Perceptual stability is also critical; small frame to frame fluctuations can produce visible jitter and motion sickness, motivating temporally smooth trajectories with low velocity and acceleration variance (Yan et al., 2021). AR sessions often last minutes to hours, demanding long term adaptation, memory management, and reliable reinitialization without drift under appearance variation, deformation, occlusion, and field of view interruptions (Yu et al., 2021). Many applications involve arbitrary user defined objects, creating an open world setting that favors category agnostic and few shot approaches over category specific models (Mayer et al., 2021). Finally, AR environments are highly interactive, with frequent occlusions and visually similar distractors that challenge appearance modeling and motion prediction, particularly in cluttered scenes (Wen et al., 2021).

2.3 Evaluation Metrics for AR-Oriented Tracking

Standard tracking benchmarks typically emphasize metrics such as center location error, intersection-over-union (IoU), success plots, and precision curves. While informative, these metrics fail to capture several aspects that are critical to AR deployment (Zhao et al., 2021). For applications involving 6-DoF tracking, pose accuracy metrics such as Average Distance of Model Points (ADD) and ADD(-S) are widely used. However, in AR contexts, spatial consistency across time is often more important than instantaneous pose error, particularly for maintaining stable virtual overlays (Mayer et al., 2022). Temporal stability can be quantified using trajectory-based metrics, including velocity variance, acceleration variance, or jerk. These measures provide a more direct proxy for perceptual smoothness than frame-wise accuracy and are essential for evaluating AR tracking quality (Cui et al., 2022). The time required to achieve stable tracking after initialization or re-detection is critical for user experience. Prolonged initialization delays or unstable recovery behavior can significantly disrupt interaction (Gao et al., 2022). Energy usage measured on target hardware platforms is an increasingly important evaluation criterion. Sustained high power consumption may lead to thermal throttling, degraded performance, or reduced battery life, all of which negatively impact AR usability.

2.4 Why Object Tracking for AR Is Fundamentally Different from Generic Tracking

Although AR tracking builds upon advances in generic visual tracking, several fundamental differences distinguish it as a separate research problem (Chen et al., 2022). First, AR tracking operates in a closed-loop system where tracking errors directly influence rendering and user interaction. In contrast, generic tracking benchmarks are open-loop and offline, with no perceptual feedback. Second, AR prioritizes perceptual stability over benchmark accuracy. A tracker that achieves high IoU scores but exhibits temporal jitter may perform poorly in AR, while a slightly less accurate but smoother tracker may deliver superior user experience. Third, AR deployment emphasizes end-to-end system constraints rather than algorithmic efficiency in isolation. Latency, power consumption, and hardware compatibility are first-order design objectives, not secondary considerations. Finally, AR tracking must generalize to open-world scenarios and arbitrary objects, often under prolonged and interactive use. These requirements fundamentally reshape both algorithm design and evaluation methodology (Paul et al., 2022). Together, these distinctions motivate treating AR-oriented object tracking as a distinct research domain, in which algorithmic accuracy, temporal stability, and system-level efficiency must be jointly optimized.

3. Deep Learning Tracking Paradigms and Their Suitability for AR

Deep learning has fundamentally transformed visual object tracking by enabling data-driven representation learning and robust modeling under complex real-world conditions. Over the past decade, several major tracking paradigms have emerged, each reflecting different design philosophies regarding efficiency, adaptability, temporal modeling, and robustness (Chen et al., 2023). When deployed in augmented reality (AR) systems, however, the performance of these paradigms must be evaluated not only in terms of tracking accuracy on standard benchmarks, but also with respect to latency, energy consumption, perceptual stability, and long-term reliability.

In this section, we systematically review four major deep learning based tracking paradigms: Siamese networks, deep discriminative correlation filters, Transformer based architectures, and long term tracking frameworks, and analyze their respective strengths and limitations from an AR oriented, system level perspective.

Table 1. Comparison of Major Deep Learning Tracking Paradigms under AR-Specific Constraints

Tracking Paradigm	Representative Methods	Latency & Throughput	Energy Efficiency	Temporal Stability	Long-Term Robustness	Adaptability	AR Deployment Suitability
Siamese Networks	SiamFC; SiamRPN(++); SiamMask; Ocean; LightTrack	Very low latency; high FPS; predictable inference	High, especially with lightweight backbones	Moderate; may suffer from drift and jitter	Limited without explicit re-detection	Low; primarily offline trained	Well-suited for short-term, interaction-intensive AR scenarios where responsiveness is critical
Deep DCF-based Trackers	ECO; ATOM; DiMP;	Moderate latency due	Medium;	High if updates are	Strong under gradual	High via online learning	Suitable for long-duration AR sessions,

	PrDiMP	to online updates	update cost is non-negligible	well-regularized	appearance change		but requires stability-aware update control
Transformer-based Trackers	TransT; STARK; OSTrack; MixFormer; SimTrack	Historically high, now moderate with lightweight designs	Medium to low; improving with efficient attention	High; global context modeling reduces jitter	Strong under occlusion and clutter	Medium; mostly offline with limited adaptation	Promising for complex AR scenes, requires hardware-aware optimization
Long-Term Tracking Frameworks	LTMU; SPLT; GlobalTrack variants	Variable; re-detection introduces latency spikes	Medium to low	Variable; depends on memory and update strategy	Very high; handles target disappearance	Medium to high	Essential for persistent AR anchoring, should be tightly integrated with SLAM
Emerging Architectures	State-space models; diffusion-based trackers	Uncertain; mostly prototype-level	Unclear	Potentially high	Potentially high	Medium	Research-stage; real-time AR applicability remains open

3.1 Siamese Network Paradigm: Efficiency-Oriented Tracking

The Siamese network paradigm represents one of the most influential and widely adopted approaches in modern object tracking. Early Siamese trackers reformulated tracking as a similarity learning problem between a target template extracted from an initial frame and a candidate search region in subsequent frames (Wen et al., 2023a), enabling efficient feed forward inference without expensive online updates. SiamFC established the foundational framework by showing that a fully convolutional Siamese network could achieve real time performance with competitive accuracy, while methods such as SiamRPN and SiamRPN++ integrated region proposal networks to improve scale and aspect ratio estimation, enhancing robustness under scale variation and fast motion common in interactive AR scenarios (Kristan et al., 2023). Recent variants explored anchor free formulations, lightweight backbones, and mobile friendly architectures (e.g., Ocean, LightTrack) to reduce computational overhead and facilitate deployment on resource constrained AR platforms such as smartphones and head mounted displays. From an AR oriented perspective, Siamese trackers benefit from predictable low latency and the absence of online learning, which simplifies system integration and avoids unstable updates (Chen et al., 2023). However, reliance on offline trained representations limits their adaptability to illumination changes, deformation, and prolonged occlusion in long duration AR sessions, and the lack of explicit recovery mechanisms hinders re acquisition after target disappearance. Consequently, Siamese trackers are well suited for short term, interaction intensive scenarios where responsiveness and stability outweigh long term adaptability, including object manipulation, gesture based interaction, and rapid scene exploration. In practice, they are often paired with higher level system components such as periodic reinitialization, detector based recovery, or SLAM constraints to mitigate drift and improve operational robustness.

3.2 Deep Discriminative Correlation Filters: Online Adaptation and Stability

Deep discriminative correlation filter (DCF) based trackers represent a complementary design philosophy that emphasizes online adaptation and discrimination between target and background. Classical DCF methods exploited frequency domain optimization, while modern deep DCF trackers integrate convolutional neural network features to improve representational power. ECO introduced efficient convolution operators and factorized convolution to enable deep feature usage without prohibitive cost, ATOM decoupled target classification from bounding box estimation for independent optimization (Wen et al., 2024), and DiMP and its variants further learned the optimization process itself, improving robustness and adaptability. Recent extensions incorporating memory mechanisms and distractor modeling allow DCF based trackers to maintain discriminative power in cluttered environments (Xie et al., 2024), a capability particularly relevant to AR scenarios involving interactive occlusions and visually similar backgrounds. The primary advantage of DCF based trackers lies in their strong adaptability; by continuously updating the appearance model during inference, they accommodate gradual changes in appearance, lighting, and context (Hong et al., 2024), making them suitable for long duration AR applications. However, online adaptation introduces challenges, as noisy or occluded observations can corrupt the model, leading to drift or failure, and the computational cost of continual optimization increases latency and energy consumption, conflicting with AR's strict real time constraints. In AR deployment, DCF based trackers are thus well suited for persistent object interaction scenarios, such as industrial inspection or maintenance, but perceptual stability demands careful regulation of update strategies through confidence estimation, temporal smoothing, or conservative scheduling to prevent perceptual jitter that is immediately noticeable to users.

3.3 Transformer-Based Tracking: Global Context and Robust Interaction

Transformer-based architectures have recently emerged as a strong alternative to convolution-centric tracking approaches. By leveraging self-attention and cross-attention, they explicitly model global dependencies between the target and its surrounding context. Early works such as TransT and STARK demonstrated the effectiveness of attention mechanisms under occlusion and background clutter (Wang et al., 2024), while later methods including OSTrack, MixFormer, and SimTrack adopted one-stream designs that unify feature extraction and matching within a single Transformer backbone for improved efficiency. Recent studies further explored lightweight and hybrid variants that combine convolutional layers with efficient attention mechanisms, token pruning, and reduced-resolution representations, lowering memory access and computational cost for mobile and edge AR platforms. Transformer-based trackers offer advantages for AR deployment, including improved robustness under partial occlusion and clutter, as well as more stable localization through broader spatial cues. However, they remain more resource-intensive than Siamese or DCF-based approaches (Ravi, et al., 2024), and attention operations may exceed latency or power budgets on mobile AR devices. In practice, Transformer-based trackers are most effective in visually complex environments that demand contextual reasoning, and real-world deployment benefits from hardware-aware attention design, selective token processing, and hybrid CNN–Transformer pipelines. With such optimizations, Transformers represent a promising direction for next-generation AR tracking.

3.4 Long-Term Tracking and Occlusion-Aware Architectures

Long-term tracking frameworks address scenarios in which targets may undergo extended occlusion, leave the field of view, or reappear after prolonged absence. These methods typically integrate short-term local tracking with global re-detection mechanisms and explicit memory components. Representative approaches combine a fast local tracker with a detector or retrieval module that searches for the target at a global scale. Memory banks storing historical target representations are often employed to maintain identity consistency over time. Long-term tracking capabilities are essential for persistent AR content anchoring, where virtual objects must remain associated with physical counterparts across interruptions. However, global re-detection and memory management introduce additional latency and complexity, which may conflict with real-time AR constraints. In AR systems, long-term tracking frameworks are most effective when tightly integrated with SLAM and spatial mapping components. Spatial constraints provided by SLAM can significantly reduce the search space for re-detection, improving efficiency and stability. Conservative memory update strategies are also critical to avoid perceptual artifacts during re-acquisition.

3.5 Emerging Architectures and AR-Oriented Design Trends (2024–2025)

Recent studies have explored alternative temporal modeling paradigms, including state space models with linear computational complexity and diffusion based approaches for robust state refinement under uncertainty (Wu et al., 2024). While these architectures show promise in offline evaluation, their real time applicability to AR remains uncertain due to computational demands and integration challenges. Across tracking paradigms, no single architecture satisfies all AR requirements: Siamese trackers excel in efficiency and responsiveness, DCF based methods offer strong adaptability, Transformer based designs provide contextual reasoning, and long term frameworks enable persistent tracking. As a result, AR oriented systems increasingly adopt hybrid approaches and negotiate trade offs among latency, perceptual stability, and robustness (Li et al., 2024).

3.6 Representative Methods and Paradigm-Level Discussion

While Sections 3.1 to 3.4 categorize tracking methods by architectural paradigms, it is also important to highlight representative design trends and recurring principles that have shaped recent progress. Across paradigms, feature representation choices play a decisive role in balancing robustness and efficiency: early Siamese trackers adopted shallow convolutional features for real time operation, later designs incorporated deeper backbones and multilevel fusion to improve discrimination, and Transformer based methods extended this trend by modeling global context through attention. In AR systems, however, maintaining a single static template is often insufficient due to long term appearance variation, motivating controlled template update strategies such as storing a small set of historical templates or selectively updating based on confidence estimates, underscoring the importance of stability aware representation management (Liang et al., 2025). Another recurring theme is temporal reasoning beyond frame to frame matching; recent methods introduce recurrent models, temporal attention, or state space formulations, which are particularly useful for AR scenarios with rapid motion or intermittent occlusion, though real time constraints favor lightweight filters or predictive motion models over heavy recurrent architectures (Cai et al., 2025). Finally, robust failure handling remains a defining challenge, with long term frameworks integrating confidence estimation and redetection modules for recovery. In AR systems, failure detection is especially critical because incorrect tracking produces visible artifacts rather than silent errors, making conservative failure detection and graceful degradation, such as temporarily freezing virtual content or switching to lower confidence rendering modes, key design principles for AR oriented deployment.

3.7 Paradigm-Level Trade-offs and Design Considerations for AR

Although deep learning based object tracking methods can be broadly categorized into distinct paradigms, their practical performance in AR systems is ultimately governed by a set of recurring trade offs (Guo et al., 2025). A primary trade off lies between computational efficiency and representational richness. Siamese based trackers prioritize streamlined architectures and predictable inference latency, making them attractive for latency sensitive AR applications, but their limited online adaptability can hinder robustness under long term appearance variation. In contrast, Transformer based trackers offer rich contextual reasoning and improved robustness in complex scenes, yet require careful architectural optimization to satisfy mobile deployment constraints (Liu et al., 2025). Another key trade off concerns adaptability versus stability. Trackers with aggressive online update mechanisms, such as deep DCF based approaches, can rapidly adapt to evolving appearance and background conditions, but in AR systems such adaptability must be regulated to avoid perceptual instability (Sun et al., 2025), motivating conservative update strategies, confidence aware learning, and bounded memory mechanisms. Long term tracking frameworks introduce an additional trade off between robustness and system complexity: global redetection and memory mechanisms enable persistent object anchoring across interruptions, but increase latency variance and integration complexity, costs that must be weighed against persistence benefits in interactive or safety critical AR applications (Videnovic, et al., 2025). Collectively, these trade offs highlight that AR oriented tracking design is inherently application dependent, and that effective systems tailor tracking architectures and update strategies to the specific latency, stability, and robustness requirements of the target application.

Table 2. Representative Deep Learning-Based Trackers for AR-Oriented Deployment

Method	**Year**	**Paradigm**	**Key Design Characteristics**	**Strengths for AR**	**Limitations**
SiamFC	2016	Siamese	Fully convolutional similarity matching	Ultra-low latency; predictable inference	Limited adaptability; weak long-term robustness
SiamRPN++	2019	Siamese	Deep backbone with region proposal	Accurate localization with high speed	Increased computation; offline-only adaptation
DiMP	2019	DCF-based	Learned discriminative model update	Strong adaptability to appearance change	Online updates may cause instability
ATOM	2019	DCF-based	Target classification and IoU prediction	Stable tracking under gradual variation	Moderate latency and energy cost
OSTrack	2022	Transformer	One-stream Transformer architecture	Robust under occlusion and clutter	Higher memory and compute demand
MixFormer	2022	Transformer	Iterative mixed attention mechanism	Strong global context modeling	Less suitable for low-power devices
FoundationPose	2024	6-DoF Tracking	Unified pose estimation and tracking	Accurate spatial anchoring for AR	Complex pipeline; heavy computation

4. AR-Oriented Optimization and System Integration

While advances in tracking algorithms form the foundation of AR perception, practical deployment hinges on system-level optimization and tight integration with other AR subsystems. Unlike offline tracking benchmarks, AR systems operate under strict real-time, energy, and stability constraints, requiring holistic co-design across algorithms, hardware, and software.

4.1 Extreme Model Efficiency Optimization

Achieving real-time performance on mobile and edge AR platforms necessitates aggressive efficiency optimization beyond conventional FLOP reduction. In practice, end-to-end latency, memory access patterns, and power consumption are often more informative objectives than theoretical computational complexity. Hardware-aware neural architecture search has emerged as an effective strategy for tailoring tracking models to specific AR devices (Shim et al., 2025). By incorporating latency and energy measurements into the optimization objective, such approaches can produce architectures that outperform manually designed networks under real deployment conditions. Dynamic inference techniques, including adaptive resolution processing, early exiting, and confidence-aware computation, further enable trackers to allocate resources selectively based on scene complexity. Platform-specific optimization is equally critical. Efficient utilization of mobile GPUs, NPUs, and heterogeneous computing units can substantially reduce latency and energy consumption. For AR systems, these optimizations must be evaluated holistically, as improvements in one subsystem may introduce bottlenecks or synchronization issues elsewhere in the pipeline (Alansari et al., 2025).

4.2 End-to-End 6-DoF Object Pose Tracking

Many AR applications require full 6-DoF object pose tracking rather than two-dimensional localization. Recent work has explored end-to-end learning approaches that directly regress object pose from image sequences, as well as hybrid methods that combine explicit geometric models with learned feature representations (Kristan et al., 2024). End-to-end approaches offer conceptual simplicity and robustness to appearance variation, but often incur high computational cost (Wen et al., 2023b). Hybrid methods leverage geometric constraints to improve efficiency and stability, making them more suitable for real-time AR deployment. Nonetheless, maintaining sub-pixel accuracy and temporal smoothness under strict latency constraints remains a significant challenge.

4.3 Tight Coupling with SLAM and Scene Understanding

Object tracking in AR rarely operates in isolation. Tight integration with simultaneous localization and mapping (SLAM) systems enables improved global consistency and robustness. By sharing spatial constraints, tracking estimates can be stabilized using camera pose information, while tracked objects can serve as semantic landmarks for mapping. However, such coupling introduces new challenges. Errors in one module may propagate to others, amplifying failure modes (Zhang et al., 2023). Synchronization between tracking, SLAM, and rendering pipelines is also non-trivial, particularly under asynchronous sensor input. Designing robust interfaces and fallback strategies is therefore essential for reliable AR systems.

4.4 Multimodal Perception Fusion

Modern AR platforms increasingly incorporate multiple sensing modalities, including RGB-D cameras, inertial measurement units (IMUs), and event-based sensors. Multimodal fusion enhances robustness under challenging conditions such as motion blur, low illumination, and rapid motion. Effective fusion strategies must account for differing noise characteristics, temporal resolutions, and failure modes across modalities (Hodan et al., 2023). Probabilistic and confidence-aware fusion frameworks are particularly promising, as they allow the system to weigh sensor inputs dynamically based on reliability estimates.

4.5 System-Level Design Guidelines for AR-Oriented Tracking

Several system level guidelines emerge for AR oriented tracking. End to end latency must be minimized and predictable, favoring architectures with deterministic execution rather than data dependent computation spikes. Perceptual stability should be treated as a primary objective through temporal smoothing, confidence aware updates, and trajectory regularization while accounting for interactions between tracking, rendering, and user motion. Adaptation is essential for long term robustness but should be controlled via selective updates, bounded memory, and confidence thresholds. Tight integration with SLAM and scene understanding improves global consistency, yet coupling must be designed to prevent cascading failures, motivating modular interfaces, redundancy, and fallback mechanisms. Finally, AR oriented tracking should be evaluated not only by algorithmic metrics but also by human centric criteria, as user studies and perceptual experiments reveal insights beyond benchmark performance.

4.6 System-Level Failure Modes and Practical Lessons from AR Deployment

Beyond algorithmic performance, real-world AR deployment exposes several system-level failure modes that are often underrepresented in tracking benchmarks. Delayed or unstable initialization may disrupt interaction, prompting practical systems to adopt fast and conservative initialization strategies. During prolonged operation, small errors can accumulate and cause spatial misalignment of virtual content, necessitating periodic re-alignment via SLAM or environmental anchors. Latency spikes constitute another critical failure mode, as data-dependent computation or scheduling delays may break the real-time rendering loop; in such cases, worst-case latency matters more than average throughput and motivates bounded-complexity designs. Finally, failure recovery behavior strongly affects perceived robustness: abrupt re-initialization or incorrect re-detection can be visually disturbing, while graceful degradation techniques such as freezing virtual content, fading overlays, or signaling low confidence help maintain a stable and user-centric AR experience.

5. Datasets and Evaluation Protocols

Datasets and evaluation protocols play a central role in shaping the development of object tracking algorithms. However, a critical gap remains between widely used tracking benchmarks and the practical requirements of augmented reality (AR) deployment. This section reviews representative datasets from both generic tracking and AR-related domains, and analyzes their limitations from an AR-oriented perspective.

5.1 Generic Object Tracking Benchmarks

Classical object tracking benchmarks, including OTB, VOT, LaSOT, GOT-10k, and TrackingNet, have been instrumental in driving progress in deep learning–based tracking. These datasets typically emphasize short- to medium-length video sequences, diverse object categories, and standardized evaluation metrics such as precision and success curves. As a result, they provide a useful testbed for measuring algorithmic robustness under challenges such as occlusion, fast motion, and background clutter. Nevertheless, from an AR deployment perspective, these benchmarks exhibit several limitations. First, most sequences are relatively short and do not capture the long-term temporal dynamics characteristic of extended AR sessions. Second, evaluation is conducted offline and open-loop, without accounting for feedback from rendering or user interaction. Third, the metrics prioritize frame-wise accuracy rather than perceptual stability, making it difficult to assess jitter, drift, or latency-induced artifacts that are critical in AR systems.

5.2 6-DoF Object Pose Estimation and Tracking Datasets

For AR applications that require spatial anchoring of virtual content to physical objects, 6-DoF object pose tracking is often more relevant than two-dimensional bounding box tracking. The BOP benchmark series has become a standard evaluation framework for object pose estimation, providing multiple datasets, unified metrics, and reproducible evaluation protocols. While BOP-style datasets are valuable for benchmarking pose accuracy, they often assume controlled capture conditions and limited interaction. Occlusion patterns are typically synthetic or static, and long-term temporal consistency is not a primary evaluation target. As a result, high performance on pose benchmarks does not necessarily translate to perceptually stable AR experiences under real-world usage.

5.3 Emerging AR-Specific and Multimodal Datasets

Recent research has begun to address these gaps by introducing datasets tailored to AR deployment scenarios. Such datasets increasingly incorporate long sequences, handheld or head-mounted camera motion, multimodal sensing (e.g., RGB-D and IMU), and realistic interaction patterns involving hands and tools. These characteristics better reflect the challenges faced by AR tracking systems in practice. Despite this progress, publicly available AR-specific datasets remain limited in scale and diversity. Many datasets are collected using proprietary platforms or restricted environments, hindering reproducibility and fair comparison. Expanding the availability of open, large-scale AR tracking datasets therefore remains an important research priority.

5.4 Evaluation Beyond Accuracy: Toward AR-Relevant Metrics

From an AR-oriented perspective, evaluation protocols must move beyond conventional accuracy metrics. Temporal consistency measures, such as velocity or acceleration variance, provide a more direct proxy for perceptual smoothness. Initialization and recovery latency should also be evaluated explicitly, as delayed or unstable recovery can severely disrupt user interaction. Energy consumption and thermal behavior are additional factors that are rarely considered in tracking benchmarks but are critical for sustained AR operation. Incorporating such metrics into standardized evaluation protocols would significantly improve the relevance of benchmark results for real-world AR deployment.

6. Open Challenges and Future Research Directions

Despite substantial progress in deep learning based object tracking, reliable large scale AR deployment remains challenging. A central issue is robust generalization under open world conditions, where trackers must handle unseen objects, maintain identity over time, and avoid drift under occlusion and appearance variation. Beyond accuracy, AR systems require a joint optimization of accuracy, temporal stability, and computational efficiency, motivating multi objective training and evaluation frameworks that explicitly capture these trade offs. A significant gap also persists between state of the art tracking algorithms and deployable AR systems, as many methods are evaluated in isolation without considering synchronization, memory constraints, or interaction with SLAM and rendering pipelines. As AR applications move toward safety critical and professional domains, trustworthiness becomes essential, with an increasing need for confidence estimates, uncertainty modeling, and interpretable failure signals evaluated through human centric studies. Looking forward, integrating tracking into broader world models that capture dynamics, semantics, and physical constraints may enable predictive tracking, more robust recovery, and deeper interaction capabilities, suggesting that future progress will depend on holistic approaches that unify algorithmic advances with system level design.

7. Conclusion

Deep learning based object tracking has become a core capability for modern AR systems, determining how virtual content is spatially anchored, temporally stabilized, and perceptually integrated with the physical world. Unlike generic tracking, AR oriented tracking must satisfy stringent system level constraints, including tight latency and energy budgets, long term operation, and strong sensitivity to perceptual instability. This survey has examined recent advances from a system oriented AR perspective and analyzed four major tracking paradigms, highlighting their respective strengths, limitations, and deployment trade offs. Our discussion underscores that benchmark accuracy alone is insufficient for AR deployment; temporal stability, interaction robustness, and predictable computational behavior are equally essential. No single paradigm currently satisfies the diverse requirements of AR, motivating hybrid designs, controlled adaptation strategies, and tighter coupling with complementary modules such as SLAM and multimodal sensing. We argue that AR oriented tracking constitutes a distinct research domain that requires holistic approaches integrating algorithmic accuracy, perceptual stability, and system efficiency, as well as closer collaboration between vision, systems, and HCI. By consolidating recent progress and outlining open challenges, this survey provides a structured reference and research roadmap for next generation AR tracking systems.

References

Alansari M, Hassan M, et al. (2025) 'Visual tracking by matching points using diffusion models', *Future Generation Computer Systems*, 152, pp. 98–110.

Cai W, Liu Y, et al. (2025) 'SPMTrack: Spatio-temporal parameter-efficient fine-tuning with mixture of experts for scalable visual tracking', In: *Proceedings of the IEEE/CVF Conference on Computer Vision and Pattern Recognition*, pp. 10452–10461.

Chen B, Li P, Bai L, et al. (2022) 'Backbone is all your need: A simplified architecture for visual object tracking', In: *Proceedings of the European Conference on Computer Vision*, pp. 375–391.

Chen X, Peng H, Wang D, et al. (2023) 'SeqTrack: Sequence to sequence learning for visual object tracking', In: *Proceedings of the IEEE/CVF Conference on Computer Vision and Pattern Recognition*, pp. 14535–14544.

Chen X, Yan B, Zhu J, et al. (2021) 'Transformer tracking', In: *Proceedings of the IEEE/CVF Conference on Computer Vision and Pattern Recognition*, pp. 8126–8135.

Chen Y H, Kristan M, et al. (2023) 'NeighborTrack: Single object tracking by bipartite matching with neighbor tracklets', In: *Proceedings of the IEEE/CVF Conference on Computer Vision and Pattern Recognition Workshops*, pp. 1823–1832.

Cui Y, Jiang C, Wang L, et al. (2022) 'MixFormer: End-to-end tracking with iterative mixed attention', In: *Proceedings of the IEEE/CVF Conference on Computer Vision and Pattern Recognition*, pp. 13608–13617.

Dai K, Zhang Y, Wang D, et al. (2020) 'High-performance long-term tracking with meta-updater', In: *Proceedings of the IEEE/CVF Conference on Computer Vision and Pattern Recognition*, pp. 6298–6307.

Danelljan, M., Goutam, B. and Khan, F.S. (2020) 'Probabilistic regression for visual tracking', In: *Proceedings of the IEEE/CVF Conference on Computer Vision and Pattern Recognition (CVPR)*, pp. 7183–7192.

Gao S, Zhou C, Ma C, et al. (2022) 'AiATrack: Attention in attention for transformer visual tracking', In: *Proceedings of the European Conference on Computer Vision*, pp. 282–299.

Guo M, Zhang R, et al. (2025) 'DreamTrack: Dreaming the future for multimodal visual object tracking', In: *Proceedings of the IEEE/CVF Conference on Computer Vision and Pattern Recognition*, pp. 11234–11243.

Hodan T, Sundermeyer M, Drost B, et al. (2020) 'BOP Challenge 2020 on 6D object localization', In: *Proceedings of the European Conference on Computer Vision Workshops*, pp. 577–594.

Hodan T, Sundermeyer M, et al. (2023) 'BOP Challenge 2022 on detection, localization and pose estimation', *International Journal of Computer Vision*, 131(8), pp. 1940–1962.

OPEN ACCESS

Hong L, Wang Z, et al. (2024) 'OneTracker: Unifying visual object tracking with foundation models and efficient tuning', In: *Proceedings of the IEEE/CVF Conference on Computer Vision and Pattern Recognition*, pp. 16412–16421.

Kristan M, Leonardis A, Matas J, et al. (2023) 'The VOTS2023 challenge results', In: *Proceedings of the IEEE/CVF International Conference on Computer Vision Workshops*, pp. 312–331.

Kristan M, Leonardis A, Matas J, et al. (2024) 'The visual object tracking challenge 2024 results', In: *Proceedings of the IEEE/CVF Conference on Computer Vision and Pattern Recognition Workshops*, pp. 1–15.

Labbé Y, Carpentier J, Aubry M, et al. (2020) 'CosyPose: Consistent multi-view multi-object 6D pose estimation', In: *Proceedings of the European Conference on Computer Vision*, pp. 574–591.

Li Y, Zhang H, et al. (2024) 'A transformer-based visual object tracker via learning immediate appearance change information in videos', *Pattern Recognition*, 148, pp. 110125.

Liang S, Chen Z, et al. (2025) 'Autoregressive sequential pretraining for visual tracking', In: *Proceedings of the IEEE/CVF Conference on Computer Vision and Pattern Recognition*, pp. 9231–9240.

Liu X, Wang Y, et al. (2025) 'MambaVLT: Time-evolving multimodal state space model for vision-language tracking', In: *Proceedings of the IEEE/CVF Conference on Computer Vision and Pattern Recognition*, pp. 12801–12810.

Mayer C, Danelljan M, Paudel D P, et al. (2021) 'Learning target candidate association to keep track of what not to track', In: *Proceedings of the IEEE/CVF International Conference on Computer Vision*, pp. 13444–13454.

Mayer C, Danelljan M, Paudel D P, et al. (2022) 'Transforming model prediction for tracking', In: *Proceedings of the IEEE/CVF Conference on Computer Vision and Pattern Recognition*, pp. 8731–8740.

Paul M, Danelljan M, Van Gool L, et al. (2022) 'Robust visual tracking by segmentation', In: *Proceedings of the European Conference on Computer Vision*, pp. 571–588.

Ravi N, et al. (2024) 'SAM 2: Segment anything in images and videos', In: *Proceedings of the IEEE/CVF Conference on Computer Vision and Pattern Recognition*, pp. 4012–4021.

Shim K, Lee S, et al. (2025) 'Focusing on tracks for online multi-object tracking', In: *Proceedings of the IEEE/CVF Conference on Computer Vision and Pattern Recognition*, pp. 14903–14912.

Sun C, Zhao J, et al. (2025) 'Exploring historical information for RGBE visual tracking with Mamba', In: *Proceedings of the IEEE/CVF Conference on Computer Vision and Pattern Recognition*, pp. 13592–13601.

Videnovic J, et al. (2025) 'A distractor-aware memory for visual object tracking with SAM2', In: *Proceedings of the IEEE/CVF Conference on Computer Vision and Pattern Recognition*, pp. 14122–14131.

Wang N, Zhou W, Wang J, et al. (2021) 'Transformer meets tracker: Exploiting temporal context for robust visual tracking', In: *Proceedings of the IEEE/CVF Conference on Computer Vision and Pattern Recognition*, pp. 15711–15720.

Wang X, Zhang Y, et al. (2024) 'Event stream-based visual object tracking: A high-resolution benchmark dataset and evaluation', In: *Proceedings of the IEEE/CVF Conference on Computer Vision and Pattern Recognition*, pp. 11983–11992.

Wen B, Yang W, Birchfield S, et al. (2021) 'BundleTrack: 6D pose tracking for novel objects without instance or category-level 3D models', In: *Proceedings of the IEEE/RSJ International Conference on Intelligent Robots and Systems*, pp. 806–813.

Wen B, Yang W, Kautz J, et al. (2023a) 'BundleSDF: Neural 6-DoF tracking and 3D reconstruction of unknown objects', In: *Proceedings of the IEEE/CVF Conference on Computer Vision and Pattern Recognition*, pp. 15861–15870.

Wen B, Yang W, Kautz J, et al. (2023b) 'Neural object-centric tracking and reconstruction in the wild', In: *Proceedings of the IEEE/CVF International Conference on Computer Vision*, pp. 18456–18465.

Wen B, Yang W, Kautz J, et al. (2024) 'FoundationPose: Unified 6D pose estimation and tracking of novel objects', In: *Proceedings of the IEEE/CVF Conference on Computer Vision and Pattern Recognition*, pp. 14291–14300.

Wu J, Jiang Y, Liu Q, et al. (2024) 'General object foundation model for images and videos at scale', In: *Proceedings of the IEEE/CVF Conference on Computer Vision and Pattern Recognition*, pp. 5123–5132.

Xie F, Wang C, Wang G, et al. (2024) 'DiffusionTrack: Point set diffusion model for visual object tracking', In: *Proceedings of the IEEE/CVF Conference on Computer Vision and Pattern Recognition*, pp. 8751–8760.

Yan B, Peng H, Wu K, et al. (2021) 'Learning spatio-temporal transformer for visual tracking', In: *Proceedings of the IEEE/CVF International Conference on Computer Vision*, pp. 10448–10457.

Yu B, Tang M, Zheng L, et al. (2021) 'High-performance discriminative tracking with transformers', In: *Proceedings of the IEEE/CVF International Conference on Computer Vision*, pp. 9854–9863.

Zhang T, Huang L, et al. (2023) 'Unified multimodal tracking with event cameras and RGB sensors', In: *Proceedings of the IEEE/CVF International Conference on Computer Vision*, pp. 19342–19351.

Zhao M, Okada K, Inaba M. (2021) 'TrTr: Visual tracking with transformer', In: *Proceedings of the IEEE/CVF International Conference on Computer Vision Workshops*, pp. 156–165.

Disclaimer/Publisher's Note: The statements, opinions and data contained in all publications are solely those of the individual author(s) and contributor(s) and not of Brilliance Publishing Limited and/or the editor(s). Brilliance Publishing Limited and/or the editor(s) disclaim responsibility for any injury to people or property resulting from any ideas, methods, instructions or products referred to in the content.

Spatial Design Strategies for the China Industrial Design Museum from the Perspective of Functional Integration

Xu Dan[1,2*], Rahah bt. Hasan[1], Wang Yuqi[2]

[1] Faculty of Applied and Creative Arts, University Malaysia Sarawak, Malaysia
[2] Faculty of Design & Art, Yancheng Institute of Technology, Yancheng, Jiangsu, China
* Correspondence: 195290014@qq.com

https://doi.org/10.53104/j.acad.res.adv.2026.03002

Abstract: Against the backdrop of cultural industry upgrading and urban regeneration, the single-function model of design museums can no longer meet diversified public needs. This study takes the China Industrial Design Museum as the research object, aiming to explore the spatial optimization strategy for functional integration. Based on literature review, field investigation and in-depth interviews, this study systematically analyzes the spatial layout, functional structure, operation mode and visitor experience of the museum. The results show that the museum has a professional collection system and clear positioning, but still faces prominent problems such as insufficient functional synergy, monotonous circulation design, weak interactive experience and lack of auxiliary spaces. Multiple functions are simply superimposed rather than organically integrated. To solve these problems, this study constructs three functional integration modes: collection-culture inheritance, exhibition-community service, and education-research-industry renewal. Four design principles are proposed, namely functional collaboration, spatial adaptability, experience priority and sustainable development. Furthermore, this study puts forward a phased spatial optimization scheme from the aspects of circulation reconstruction, functional zoning, material selection and exhibition system optimization. This study enriches the theoretical system of spatial design of professional design museums, and provides practical reference for functional upgrading and spatial renewal of similar museums.

Keywords: functional integration; design museum; spatial design; China industrial design museum

Received: 23 April 2026

Revised: 30 April 2026

Accepted: 6 May 2026

Published: 8 May 2026

Citation: Xu, D., Hasan, R. bt. and Wang, Y. (2026) 'Spatial Design Strategies for the China Industrial Design Museum from the Perspective of Functional Integration', *Journal of Academic Research and Advances*, 2(1), pp. 15-34.

Copyright: © 2026 by the authors. This article is an open access article distributed under the terms and conditions of the Creative Commons Attribution (CC BY) license (https://creativecommons.org/licenses/by/4.0/).

1. Introduction

1.1 Research Background

Rapid social progress and rising public cultural demands have continuously driven design museums to explore new development paths (Zhang Jin, 2004). Functional integration has emerged as a critical trend, breaking the traditional single-function exhibition-oriented pattern by organically combining exhibition, education, research, communication, and leisure to deliver diversified visitor experiences (Zhou Jie, 2012). As iconic urban cultural and creative landmarks, design museums also shoulder multiple social responsibilities, including cultural transmission, public education, industrial empowerment, and urban image enhancement (Chen Ming, 2020). Such roles require spatial functions to transcend the conventional mono-functional model and achieve synergistic integration of multiple purposes.

1.2 Research Significance

1.2.1 Theoretical Significance

First, this study enriches the theoretical system of spatial design for design museums. By deeply integrating the concept of functional integration with spatial design in design museums, it clarifies the core logic, theoretical framework, and design principles of spatial design in design museums from the perspective of functional complexity, and makes up for the lack of interdisciplinary research between current spatial design in design museums and the theory of functional complexity from a new perspective.

Second, it supplements the application theory of the concept of functional complexity in public cultural spaces. Taking the China Industrial Design Museum as a specific case, this study deeply analyzes the application paths, existing problems, and optimization directions of the concept of functional complexity in the space of design museums, and provides a theoretical reference for the application of the theory of functional complexity in similar public cultural spaces.

Third, it sorts out the classification types and spatial characteristics of design museums, constructs a suitable theoretical framework for functional complex spatial design, and enriches the connotation of classification research and spatial design theory of design museums.

1.2.2 Practical Significance

First, focusing on the China Industrial Design Museum, this study conducts an in-depth investigation into the current state of its spatial-functional integration, identifies existing problems and deficiencies, and proposes targeted optimization strategies. These strategies aim to improve its spatial layout, enhance functional synergy, and strengthen visitor experience, thereby further enabling the museum to fulfill its roles in cultural dissemination and industrial empowerment, and enhance its influence within the sector.

Second, for the contemporary design museum industry, the proposed spatial design strategies for functional integration offer applicable practical solutions for spatial design and functional upgrading of various design museums—especially private and sector-specific ones. These solutions help address developmental challenges such as single-function structures and insufficient visitor experiences, and promote high-quality development of the design museum industry.

2. Theoretical Foundations

2.1 Theories Related to Design Museums

2.1.1 Definition of the Design Museum

According to Wikipedia, a design museum centers on product, industrial, graphic, fashion, and architectural design. Most existing design museums focus primarily on applied and decorative arts, with collections dating mainly from the twentieth century onward.

In this study, a design museum is defined as an institution centered on design culture, dedicated to the collection, exhibition, research, education, and promotion of design works, processes, ideas, and impacts (Li Huizhu, 2003). Its core characteristics include: taking design as its central theme, covering industrial design, graphic design, fashion design, environmental design, and other fields; integrating artistic and practical values, emphasizing the close links between design, daily life, society, and industry (Liu Guanzhong, 2018); emphasizing the presentation of design processes and the dissemination of design thinking rather than merely the aesthetic value of finished works; and featuring strong practicality and participation, encouraging public understanding and engagement through interactive experiences.

In summary, the design museum in this paper is a non-profit permanent cultural institution with design as its core theme. It integrates systematic collection, academic research, public exhibition, educational communication, and innovative empowerment. It focuses on diverse design works and design culture, connects history, the present, and the future, and promotes design exchange and industrial development. Its core values are to inherit design culture, popularize design knowledge, stimulate design innovation, and support the deep integration of design with society, culture, and technology.

2.1.2 Core Functions of the Design Museum

The spatial functions of a design museum reflect its core values. With social progress, its spatial functions have evolved from the traditional single focus on collection and exhibition toward diversified integration. Based on the positioning and requirements of design museums, four core spatial functions are identified:

1) Collection and Exhibition

Collection is the most fundamental function of a design museum and the foundation of all museum activities. It mainly collects and preserves various design works, manuscripts, tools, and archives, and presents design achievements and developmental histories to the public through scientific curation. Exhibition focuses not only on the presentation of exhibits but also on the creation of an appropriate spatial atmosphere. Spatial design, lighting design, and circulation planning are used to enhance the appreciation and communication effects of exhibits. The term "collection" is commonly used to distinguish museum acquisitions from other forms of gathering. Museum collections are defined as objects preserved for their representative, referential, aesthetic, or educational significance. Therefore, for design museums, systematic collection of design works is the top priority.

2) Education and Research

Education is one of the core social functions of museums. The development of contemporary museums relies on the renewal of educational concepts and the innovation of educational activities. As an important carrier for the dissemination of design culture, design museums perform two major functions: public education and design research (Xin Yihua & Tu Le, 2012).

In terms of educational function, design museums provide differentiated values for different groups. For design students, they enable close observation and in-depth study of classic works, consolidating professional knowledge. For primary and secondary school students and non-professional audiences, they help to build basic design literacy and enrich spiritual and cultural life. In addition, design museums can popularize design knowledge and cultivate public design awareness through public activities such as lectures, art salons, and youth design courses.

In terms of research function, design museums undertake important academic missions. On the one hand, they provide professional research platforms for designers and researchers to support theoretical research, historical studies, and innovative practices, thereby promoting the overall development of the design industry. On the other hand, their research scope also includes the summary and optimization of their own operation and management models, as well as the academic deepening of the design discipline, thus achieving the mutual improvement of design professional development and museum institutional operation.

2.2 Theories of Functional Integration

2.2.1 Connotations and Characteristics of Functional Integration

Functional integration refers to the integration of multiple distinct functions within a single spatial setting, enabling them to operate in a mutually supportive manner. This approach transcends the limitations of single-function spaces, enhances spatial efficiency, value, and user experience, and responds to diverse contemporary demands. Crucially, functional integration does not entail the mere superimposition of functions; instead, it emphasizes interfunctional correlation and mutual reinforcement. Through rational spatial programming, diverse functions are synthesized into an organic, cohesive whole.

In alignment with the characteristics of architectural spatial design, functional integration presents four core characteristics:

1) Plurality: Hybrid spaces accommodate multiple functions to satisfy contextual diversity. For instance, a design museum integrates exhibition, education, communication, and recreation within a unified spatial framework.

2) Synergy: Functions operate interactively rather than in isolation. Through deliberate design, interfunctional reinforcement elevates overall spatial value. In museums, exhibition functions provide content for educational activities, while educational interpretation deepens audience engagement with exhibits.

3) Flexibility: Hybrid spaces demonstrate high adaptability, with adjustable functions and layouts to respond to evolving scenarios and demands. Multi-purpose halls in design museums can be reconfigured for lectures, seminars, workshops, or temporary exhibitions.

4) Efficiency: Integrated programming optimizes spatial utilization, reduces redundant construction, and lowers operational costs, maximizing spatial value. The combination of visitor lounges and museum retail zones enhances both convenience and commercial vitality.

2.2.2 Principles of Functional Integration in Spatial Design

The application of functional Integration follows three core principles: demand-orientation, systematic programming, and symbiotic synergy.

1) Demand-orientation principle: The essence of functional integration is to satisfy diverse human needs. Spatial programming must identify user groups, behavioral patterns, and contextual demands to align functions with expectations. In design museums, users include general visitors, practitioners, researchers, and students, requiring integrated systems of collection, exhibition, education, and research.

2) Systematic programming principle: Hybrid spaces constitute an organic system with close interrelationships between functional zones. Design must rationalize spatial boundaries, optimize circulation, and ensure seamless transitions between zones. In design museums, exhibition, education, and communication zones are hierarchically organized to form fluent visitor circulation.

3) Symbiotic synergy principle: Diverse functions are designed to mutually reinforce and enhance one another, generating greater value than isolated operations. In museum settings, exhibition areas attract audiences; retail and educational zones extend engagement; research outcomes enrich content; and educational activities disseminate research.

2.2.3 Application of Functional integration in Museums

Functional integration is a trans-disciplinary theory integrating mathematics, engineering, product design, and architecture. Its theoretical core is to transcend the boundaries of single-function models, systematically integrate diverse functional units, and construct holistic, synergistic, and adaptive systems. This achieves 1+1>2 synergistic effects and maximizes resource utilization, representing an evolutionary shift from fragmentation to integration.

In museum contexts, functional integration denotes the organic integration of historically discrete functions—collection, preservation, research, exhibition, education, and public service—into a unified operational system. This represents a developmental shift from closed, mono-functional institutions to open, multi-dimensional cultural platforms.

Drivers of functional integration include:

Audience demand: Diversified visitor expectations, elevated cultural literacy, and changing consumption patterns require museums to support multiple activities within integrated spaces.

Institutional evolution: Museums are transforming from static repositories to dynamic public-cultural hubs.

In this study, functional integration in design museums is defined as the process and state of integrating supplementary functions—education, research, public interaction, and creative production—with core exhibition functions to form a pluralistic, synergistic, and organic system. Its theoretical core is to enhance spatial efficiency, strengthen museum-society connections, and maximize social value.

1) Functional integration manifests in three dimensions:

- Functional pluralism: Spaces simultaneously support exhibition, education, research, socialization, and creative production.
- Spatial flexibility: Morphological adaptability to respond to variable functional requirements.
- Operational synergy: Interfunctional reinforcement rather than superficial superimposition.

2) Functional integration operates at three progressive levels:

- Basic level: Integration of core exhibition with auxiliary services.
- Intermediate level: Integration of exhibition with education and research.
- Advanced level: Integration of exhibition with public services, creative industries, and community engagement.

3. Case Overview and Empirical Research

3.1 Overview of the China Industrial Design Museum

3.1.1 Location

The China Industrial Design Museum is situated within the International Industrial Design Center in Baoshan District, Shanghai. It is bordered by Songfa Road to the north, Yixian Road to the east, and Changyi Road to the south. As the first museum in China dedicated to industrial design, it showcases outstanding design works and achievements by professional designers, presenting a panoramic historical narrative of China's industrial design development and delineating a clear trajectory of China's design accomplishments, with a particular emphasis on the modern design achievements of Shanghai. The International Industrial Design Center houses the Shanghai Industrial Design Center, university-affiliated laboratories, and other functional spaces, embodying a profound design-oriented ecosystem. Moreover, the museum is surrounded by academic institutions including Fudan University and Shanghai Baoshan Vocational and Technical College, laying a solid foundation for close industry-academia collaboration. To its northeast lies the Shanghai Museum of Glass. Collectively, the China Industrial Design Museum enjoys exceptional geographical advantages for advancing integrated industry-education development (Wei Dongfeng & Sun Yu, 2007).

3.1.2 Significance of Establishment

First, the museum enables contemporary designers to move beyond a singular focus on international design history toward a dual engagement with both international design history and the history of Chinese industrial design. The historical development of Chinese industrial design has long been fragmented; the establishment of the China Industrial Design Museum therefore serves as a critical catalyst for systematic research into China's design history.

Second, the museum facilitates the creation of new industrial design products with enhanced value (Fu Yao, Liu Wenjun & Cui Yue, 2003). Rather than merely commemorating vintage industrial artifacts, the museum aims to stimulate innovative redesign practices and generate novel design outputs.

Third, it achieves a dual transformation from academic value to industrial value. Research on Chinese industrial design necessitates the integration of documentary records and physical exhibits. However, existing academic literature on

Chinese industrial design remains limited. Consequently, comprehensive research relies on a tripartite framework of physical exhibits, textual documentation, and visual archives—a core objective guiding the construction and development of the China Industrial Design Museum.

3.2 Analysis of Exhibition Spaces and Circulation

The China Industrial Design Museum presents key industrial design achievements forged along China's path toward modern industrialization from the modern and contemporary eras (Wang Shouzhi, 2016). It narrates the history of Chinese design across different periods, industries, and regions—how design responded to the demands of the times, forged ahead with proactive exploration, and contributed to the development of socialist economic construction. In addition, the museum regularly hosts a variety of programs including study tours, practical education, and Party-building outreach activities, introducing visitors to cutting-edge international design intelligence and emerging trends.

3.2.1 Functional Layout of Exhibition Spaces

Taking technological advancement and industrial design accomplishments as its curatorial narrative thread, the China Industrial Design Museum comprises four thematic halls: *Ancient Chinese Artifact Making Wisdom, The Emergence of Modern Chinese Industry, Chinese Industrial Design in Practice, and Rapidly Developing Chinese Industrial Design*. A study activity zone and a cultural and creative products zone are situated near the museum exit.

3.2.2 Analysis of Visitor Circulation

The China Industrial Design Museum is structured across two floors in accordance with its exhibition content and functional requirements.

The first floor is primarily dedicated to exhibition displays, housing the three thematic zones of *Ancient Chinese Artifact Making Wisdom, The Emergence of Modern Chinese Industry, and Chinese Industrial Design in Practice*. Adopting a loop-shaped circulation layout, it integrates the three exhibition themes coherently while accommodating the spatial needs of an open exhibition configuration and central interactive installations (Gehl J, 2002). Upon completing the first-floor tour, visitors may proceed to the second floor via stairs or elevators.

The second floor accommodates the Rapidly Developing Chinese Industrial Design exhibition zone, together with the study activity zone and cultural and creative zone.

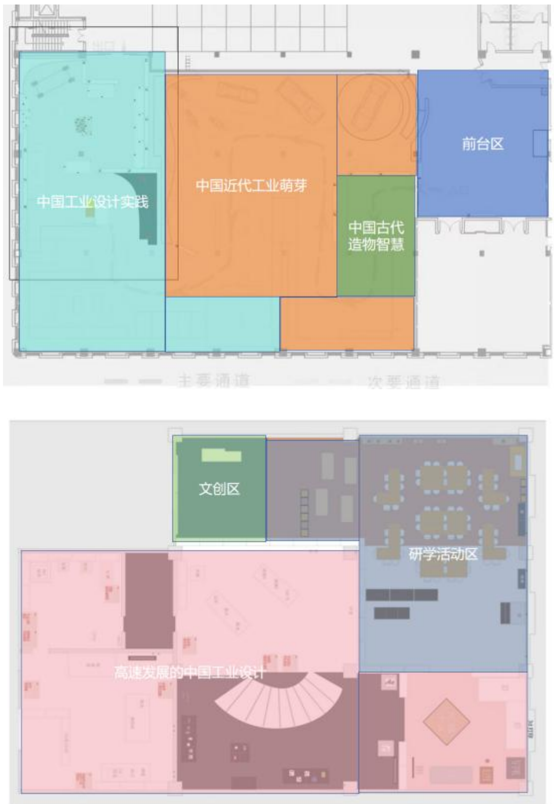

Figure 1. The Layout Plan of the China Industrial Design Museum

Source: Drawn by the author.

3.3 Exhibition Content

The China Industrial Design Museum covers an exhibition area of 3,000 square meters and is dedicated to collecting mass-produced industrial artifacts from various historical periods since the founding of the People's Republic of China in 1949. The outstanding design works currently on display illustrate the characteristics and evolutionary trajectory of Chinese industrial design from multiple perspectives, offering insights into both the wisdom of ancient Chinese design and the efforts made by modern China to pursue industrialization. By 2021, the museum's collection numbered 4,770 items (sets). Adopting a chronological narrative structure, the museum is divided into four thematic zones: Ancient Chinese Artisanal Wisdom, The Emergence of Modern Chinese Industry, Chinese Industrial Design in Practice, and The Rapid Development of Contemporary Chinese Industrial Design (Yuan Qiming, 2016).

3.3.1 Ancient Chinese Artisanal Wisdom

Located at the museum entrance, this section presents representative artifacts from different historical eras to demonstrate China's design ingenuity in agriculture, handicrafts, architecture, and related fields. Exhibits such as ancient agricultural implements, textile tools, and architectural components embody the creativity and practical wisdom of ancient laborers in production and daily life.

3.3.2 Emergence of Modern Chinese Industry

The second section focuses on the emergence of modern Chinese industry, a historical period marked by China's arduous and gradual transformation from a traditional agrarian society to a modern industrial one, embodying the profound aspirations of numerous patriots for national prosperity and rejuvenation. Centered on key historical figures and industrial artifacts and organized chronologically, this section details the state of industrial design in this era through representative exhibits, including the first 10,000-ton hydraulic forging press developed under the leadership of Shen Hong, China's first domestically built 10,000-ton vessel Dongfeng, the first 10,000-ton ocean-going cargo ship Yuejin, and Double Coin brand rubber products.

3.3.3 Chinese Industrial Design in Practice

This section traces the transformative evolution of Chinese industrial design from its inception to its growing maturity, narrating the practical endeavors forged through ingenuity and dedication. Compared with the preceding sections, it employs more diverse exhibition strategies. For instance, the Hongqi automobile display zone uses vehicles as interactive media, allowing visitors to experience their design charm through in-car engagement. Furthermore, exhibits are not presented as isolated objects but integrated into constructed contextual environments, creating an immersive viewing experience.

3.3.4 The Rapid Development of Contemporary Chinese Industrial Design

In the contemporary era, Chinese industrial design is flourishing at an unprecedented pace and has become a pivotal force driving the transformation and upgrading of China's manufacturing sector and enhancing national competitiveness. This zone displays product models accompanied by interpretive texts, combining visual and textual materials to convey design narratives effectively.

3.3.5 Activity Center and Design Studio

The final module consists of the Activity Center and Design Studio, which serve as critical platforms facilitating the museum's transition from static display to dynamic communication, with the goal of building a "living museum." As a base for science popularization and design enlightenment, the Design Studio bridges traditional craftsmanship and modern intelligent manufacturing while providing practical opportunities for university students, focusing on nurturing innovative potential for future generations. Together, these spaces transform passive viewing into deep engagement, enabling visitors to comprehend the value of design through interaction and collectively fulfilling the museum's mission of "recording history and inspiring the future."

Figure 2. The Scene of the Design Studio

Source: taken by the author.

3.4 Interview Research and Analysis

The China Industrial Design Museum (Baoshan District, Shanghai, opened in 2009), as the first museum in China dedicated to industrial design, covers an exhibition area of approximately 3,300 square meters and houses a collection of more than 4,700 exhibits. Adopting a curatorial narrative of "Industrial Prosperity—Major Manufacturing Nation—Powerful Science and Technology Country", the museum traces the evolutionary journey of Chinese industrial design from imitation and mass production to intelligent manufacturing. At present, the museum's spatial layout is dominated by static displays, characterized by single-function settings and insufficient spatial complexity. Problems such as the disconnection between exhibition and experience, inadequate public services, an imbalance between professional and public needs, and low spatial utilization efficiency have become increasingly prominent, making it difficult for the museum to fulfill its composite positioning as a venue for cultural display, science education, design communication, creative experience, and industrial services.

This study adopts a semi-structured in-depth interview approach to capture the real needs and experiential feedback of diverse stakeholders, systematically identify pain points in spatial functions, and establish a logical framework of "needs–pain points–optimization" (Zhao Jianguo, 2022), so as to provide empirical evidence for the compound functional upgrading of the museum's spatial layout.

3.4.1 Selection of Interviewees

1) Sampling Principles

This study follows a stratified sampling principle based on "core stakeholders plus diversified user groups", balancing professional visitors, general visitors, and operational staff to cover the entire chain of spatial usage. The sampling design ensures that the samples are authentic and traceable, and the data possess academic validity. A total of 45 respondents were interviewed, with each interview lasting 20–35 minutes. Interviews were conducted between September and December 2025, covering weekdays, weekends, and public holidays.

2) Classification of Interviewee Groups and Sample Composition

Table 1. Composition of Interview Samples and Sampling Rationale

Group	Number	Definition	Rationale
General Visitors	18	6 students, 7 workers, 5 seniors; 10 first-time, 8 repeat	80% of users, reflects public needs
Design Professionals	10	4 academics, 6 practitioners	Core professional users

Museum Operators	7	1 director, 2 curators, 2 guides, 2 technicians	Full operational insight
Industry Experts	5	2 museologists, 2 industrial design scholars, 1 spatial designer	Academic and industrial guidance
Young Visitors (Family)	5	3 pupils, 2 accompanying parents	Core science education group

Source: Drawn by the author.

3) Innovation in Interviewee Selection

This study breaks through the conventional single-participant model that only interviews general visitors. Instead, it integrates three-dimensional participants: museum operators, professional practitioners, and industry experts, forming a triangular validation framework among users, managers, and researchers to minimize bias in demand identification. Interviewees are further categorized by age, occupation, and visit frequency, which aligns with the composite positioning of the industrial design museum serving professional audiences, the general public, and popular science education.

3.4.2 Design of Interview Questions

1) Logical Framework

The interview protocol is structured around the core logic of spatial use – functional experience – demand pain points – optimization suggestions. Questions are divided into general modules and group-specific modules, balancing openness and pertinence. Leading questions are minimized to ensure free and authentic expression from respondents.

2) Core General Questions (for All Participants)

- What were your main purposes for visiting the China Industrial Design Museum? What functional expectations did you hold regarding the museum space prior to your visit?
- Please describe your visiting circulation. Which spaces left the deepest impression on you, and which spaces caused inconvenience or disappointment?
- In your opinion, what core functions does the current museum space possess, and what essential functions are missing?
- Among exhibition presentation, lighting, visitor circulation, and supporting facilities (rest areas, guidance, interactive installations), what are the most prominent problems?
- What composite functions should an ideal industrial design museum space provide? Please illustrate with examples.

3) Group-Specific Questions

- General Visitors

Did you have demands for rest, consultation, catering, or cultural and creative products during your visit? Can the existing space meet such needs? Is the proportion of static displays to interactive experiences reasonable? Which exhibits or zones would you like to be more interactive? Are the signage and wayfinding system clear? Did you experience disorientation or confusing circulation?

- Design Professionals

Can the space meet your needs for design research, literature access, work exchange, or small-scale seminars? What professional functions are lacking? Are the academic rigor and systematicness of the exhibitions satisfactory? Is the interpretation of exhibits and technical explanations in-depth enough? Do you require dedicated spaces for design workshops, academic salons, or industry collaboration activities?

- Museum Operators

What are the major management challenges in daily spatial operation (e.g., passenger flow guidance, functional switching, facility maintenance)? What is the functional utilization rate of the current space? Which areas are underutilized and which are overcrowded? What spatial constraints exist when holding temporary exhibitions or educational activities?

- Industry Experts

Compared with similar museums at home and abroad, what are the core shortcomings of this museum's spatial functions? How should the "composite space" of an industrial design museum be defined? What core functions must be balanced? From academic and industrial perspectives, what issues should be prioritized in spatial optimization?

- Adolescents & Parent-Child Visitors

Did you find the content and space interesting during the visit? Which parts would you like to experience hands-on? Did parents require parent-child rest areas, simple catering, or popular science interpretation? Is the existing space suitable for children and family visits?

3.4.3 Analysis of Interview Data

1) Analysis Methods

This study adopts qualitative analysis using Nvivo software combined with manual coding. The 45 transcribed interview texts were decomposed into four types of analytical units: demand descriptions, experience evaluations, pain point expressions, and optimization suggestions. Through a three-step coding procedure – open coding, axial coding, and selective coding – core dimensions were extracted. Frequency statistics were further applied to generate quantitative indicators (frequency ratio = number of mentions of a certain pain point / total number of pain point mentions). In the coding process, similar expressions in the interview transcripts were first marked as initial codes, and then grouped into broader categories such as exhibition space, public service, professional space, educational space, and spatial operation. The percentages in Table 2 indicate the relative frequency of coded pain-point mentions, rather than the proportion of respondents. Since one response may involve more than one issue, multiple coding was allowed.

2) Core Dimension Coding and Frequency Statistics

Table 2. Coding of Core Dimensions and Frequency Statistics from Interviews

Domain	Sub-code	Frequency	Ratio	Typical Quote
Exhibition Space	Static, lack of interaction	38	22.1%	"Only cases and text; no interaction to explain processes."
	Linear, weak narrative	32	18.6%	"Chronological, no story or industry logic."
	Overly technical, unbalanced	27	15.7%	"Text too professional; children cannot understand."
Public Service	Severe lack of facilities	35	20.3%	"No rest, water, or shop; experience is incomplete."
	Poor wayfinding	21	12.2%	"Confusing floors and circulation."
Professional Space	No research/communication space	19	11.0%	"No library or meeting room for research."
Educational Space	Simplistic DIY/education	15	8.7%	"Only simple T-shirts; no workshops or VR."
Spatial Operation	Inflexible layout	12	7.0%	"Cannot adapt to different events."

Source: Drawn by the author.

3) Innovation in Analytical Logic

Rather than merely listing pain points in isolation, this study combines coded quantification with typical respondent statements to clarify the relative weight and core manifestations of each issue. An analytical framework is established across five dimensions—exhibition, service, professionalism, experience, and operation—that aligns closely with the research theme of spatial functional integration.

3.4.4 Interview Results: Extraction of Core Pain Points

Based on interview analysis combined with on-site spatial investigation, five core pain points hindering the integrated functional optimization of the China Industrial Design Museum are identified:

1) Exhibition Space: Monofunctional, with Disconnection between Static Display and Design Experience

Rigid exhibition mode: 90% of respondents reported that displays are dominated by static physical objects and graphic panels, while interactive installations account for less than 5%. Only a simple DIY area is available, lacking experiential design such as AR/VR, mechanical interaction, or design process simulation. Consequently, the museum fails to reflect the core attributes of industrial design—innovation, practice, and experience (Liu Meijun & Yu Xiao, 2022).

Weak narrative logic: The exhibition route follows a strict chronological sequence without thematic, scenographic, or industrial narratives. Exhibits are presented in isolation without connecting the logical chain of design–production–life–industry. Professional visitors criticized insufficient academic depth, while general visitors found the content dull and incomprehensible.

Lack of tiered adaptation: Exhibition content and interpretive approaches do not distinguish between professional, general public, and adolescent audiences. Over-reliance on specialized text and insufficient popular science interpretation result in a triple imbalance: professionals find the content superficial, the general public struggles to understand, and adolescents show little interest.

2) Public Service Space: Functional Deficiencies, with Gaps in Basic Support and Integrated Services

Severe shortage of basic amenities: Within the 3,300-square-meter space, there are no centralized rest areas, dining zones, drinking fountains, or complete cultural and creative stores. Only a simple information desk is located at the entrance. The average visitor stay is only 1.2 hours, below the 2-hour benchmark of comparable museums, leading to a fragmented visiting experience.

Chaotic wayfinding and signage: No intelligent navigation system is available, printed guidebooks are absent, floor and exhibition zone signs are unclear, and visitor circulation lacks hierarchical routing. Congestion occurs around popular exhibits such as the Hongqi sedan, while less popular zones remain underused, resulting in highly uneven visitor distribution.

Zero functional integration: No integrated service space combining consultation, rest, cultural retail, light catering, and luggage storage has been established. Service areas are scattered and monofunctional, inconsistent with the positioning of modern museums as cultural and leisure complexes.

3) Professional Integrated Space: Functional Void, with Lack of Academic Research and Industrial Services

Absence of professional facilities: No design archive room, academic seminar room, work exchange area, or industrial collaboration hall is provided. Design students and practitioners cannot conduct research, exchanges, or seminars. The museum only fulfills a single display function and loses its core value as a service platform for the design industry.

Mixing of professional and public spaces: Professional exhibitions and public experiences are not spatially separated. No quiet dedicated research area exists, disturbing professional users and leaving their demands unmet.

Inadequate space for temporary functions: No flexible multi-purpose space is available for academic lectures, design workshops, or temporary exhibitions. Such activities can only be held in exhibition areas, disrupting regular visits and severely limiting event scale and format.

4) Experiential and Educational Space: Simplistic Forms, with Weak Popular Science Education and Creative Practice

Superficial educational experience: Science popularization relies solely on exhibit labels, with no immersive science scenarios, design practice courses, or adolescent-only experience zones. Only two to three DIY programs are offered, lacking appeal and failing to achieve the goals of integrating popularization, education, and practice (Zhu Lin, 2018).

Insufficient age-adapted design: No differentiated experiential content is designed for adolescents, middle-aged and elderly visitors, or professional groups. A one-size-fits-all spatial and content strategy renders the experience dull for young people, complicated for seniors, and superficial for professionals.

Outdated digital technology: Digital interaction and virtual simulation technologies are rarely applied. Exhibition methods remain traditional, disconnected from the curatorial theme of building a strong country through science and technology, and unable to represent the cutting-edge nature of industrial design.

5) Spatial Operation: Rigid and Inflexible, with Insufficient Flexible Adaptation and Efficient Utilization

Fixed spatial functions: The existing space consists of fixed partitions that cannot be flexibly divided, combined, or reconfigured, making it difficult to meet the integrated demands of daily exhibitions, temporary shows, academic events, and science education (Liu Jiaxing, 2018). Spatial utilization rate is only 65%, with most underused areas being marginal spaces.

Lack of separation between static and dynamic zones: Quiet exhibition areas are not effectively isolated from active experience and event zones, causing mutual interference from noise and crowds, which impairs the visiting experience and restricts event activities.

Mismatch between operation and functions: Lighting, ventilation, security, and other facilities are designed for traditional static exhibitions and cannot support interactive experiences, digital displays, or large-scale events. Facility maintenance costs are high and upgrades lag behind demand.

Based on the interview transcripts, a systematic analysis was conducted across four core dimensions: spatial function, professional experience, interactive demand, and operational service. The key findings are summarized as follows:

- Spatial Function Dimension

Most respondents endorse the museum's current positioning yet raise concerns regarding spatial coordination and layout. Approximately 80% of interviewees agree that the museum's functional positioning—integrating exhibition, research, education, and exchange—is rational and well aligned with disciplinary demands of industrial design. However, 65% perceive these functions as merely mechanically assembled rather than organically integrated, resulting in poor operational synergy. For instance, the educational activity zone is distantly separated from rest areas, making it inconvenient for visitors to rest nearby after participating in events. Furthermore, 70% of general visitors and 50% of staff members mention that auxiliary spaces including leisure zones and cultural and creative retail areas are not only undersized but also sparsely distributed, failing to accommodate diverse user needs.

- Professional Experience Dimension

Respondents from design-related professions acknowledge the museum's professional competence. Fully 90% of practitioners affirm the comprehensiveness of its collection system and the accuracy of its research orientation, noting that outcomes from the CMF Trend Laboratory hold significant industrial reference value, qualifying the museum as one of the most professionally accomplished private industrial design museums in China. Nevertheless, 75% of practitioners criticize insufficient outward communication of professional content and research findings. In-depth interpretive content related to collections remains limited, and research outputs are not effectively disseminated to the general public, creating a disconnect between research and public communication. Meanwhile, some general visitors find exhibit labels overly specialized and incomprehensible, expressing expectations for more accessible interpretations.

- Interactive Demand Dimension

Numerous respondents characterize the current interactive provision as weak and call for more diverse and professionally grounded interactive formats. A total of 85% of general visitors and 70% of practitioners report a lack of substantial interactive functions. Specifically, general visitors highlight the scarcity and simplicity of interactive devices, which are largely limited to QR-code audio guides and basic touchscreens, lacking immersive and hands-on engagement. Practitioners further argue that existing interactions are insufficiently integrated with core disciplinary attributes of industrial design, failing to convey its practical and creative nature (Wu Qiong, 2010). They recommend adding professional interactive modules such as material experience and design workshops, alongside differentiated interactive programs tailored to distinct user groups.

- Operational Service Dimension

Although most respondents express satisfaction with staff service attitudes, they also identify operational constraints and areas for improvement. Reception and interpretation services are generally regarded as professional and considerate. However, staff acknowledge unsatisfactory financial performance, a shortage of professional managerial personnel, and limited funding available for spatial renovation, equipment upgrading, and program development, all of which hinder the advancement of functional integration. Some general visitors criticize inflexible service procedures, such as cumbersome online reservation protocols and a lack of personalized interpretation services. Practitioners propose strengthening collaborations with design institutions and universities to diversify resource channels and support more professional and sustainable museum operations.

Table 3. Four-Dimensional Core Data Analysis

Dimension	Indicator	Data	Conclusion
Spatial Function	Acceptance of positioning	80%	Reasonable Position
	Poor coordination	65%	Need integration
	Dissatisfaction with auxiliary spaces	70% (visitors), 50% (staff)	Too small, scattered
Professional Experience	Professional recognition	90%	Strong expertise
	Poor outreach	75%	Research not communicated
	Technical explanations	Public feedback	Need plain language
Interactive Experience	Insufficient interaction	85% (visitors), 70% (pros)	Strong demand
	Lack of differentiation	Expert suggestion	Need audience-specific design
Operation Service	Service attitude	Mostly positive	Professional and friendly
	Funding shortage	Staff feedback	Limits upgrading
	Talent shortage	Staff feedback	Limits expansion

Source: Drawn by the author.

In summary, the analysis of interview content reveals clear discrepancies between existing conditions and stakeholder demands, providing a clear direction for subsequent on-site investigations and strategy formulation.

Operation and management staff noted that the current spatial layout is highly rigid, making functional switching difficult. Large-scale temporary events require extensive labor and time for spatial rearrangement, resulting in high operational costs.

Designers reported insufficient linkage between workshop and exhibition areas, hindering the rapid transformation of workshop outputs into exhibition content and weakening synergy between research and display.

General visitors perceived the museum's interactive experiences as monotonous, lacking opportunities for in-depth participation. Additionally, an unclear wayfinding system often causes disorientation among first-time visitors.

Park personnel expressed hopes that the museum would host more public-oriented activities for the industrial park, strengthening connections with other enterprises in the vicinity.

4. Spatial Design Strategies for the China Industrial Design Museum

4.1 Dominant Paradigms for Functional Integration in Design Museum Spaces

The mechanism of functional integration in design museums can be summarized into three major paradigms (Figure 1) (Xie Xiaoyu, 2019).

4.1.1 "Collection–Cultural Heritage" Paradigm

The "Collection–Cultural Heritage" paradigm serves as the foundational model for achieving functional integration in design museum exhibition spaces. Centered on the core function of exhibition, it integrates education, research, archiving, and other functions closely related to the communication of design culture (Li Nvxian, 2017), constructing a comprehensive platform for display, education, research, and archival preservation. Its core orientation is to better disseminate and inherit design culture, enhance public design literacy, and support the steady development of design disciplines.

- "Collection + Socialization" Integrated Scenario

Design museums may dedicate zones for social interaction, such as cafés, lounges, and plazas, where selected collections can also be exhibited, providing a public platform for communication and interaction. The integration of social and exhibition spaces weakens the quiet solemnity of traditional museums and creates a relaxed and open atmosphere for cultural exchange, greatly contributing to the inheritance of design culture. A typical example is the rooftop café and viewing terrace at the Design Museum in London, which not only offer rest and catering services but also serve as popular social venues where visitors can share impressions and design insights while enjoying urban scenery.

- "Collection + Research" Integrated Model

Design museums can establish research areas, including research rooms and archives, consolidating research resources such as design documents, sketches, and prototypes to provide a dedicated research platform for designers, scholars, and students. The integration of research and exhibition promotes the mutual transformation of research outcomes and public displays: cutting-edge findings are presented to the public through exhibitions, while public feedback gathered from exhibitions inspires new research directions. The Vitra Design Museum in Germany houses a specialized research center holding extensive design archives and collections for global design researchers, whose outputs are regularly shared with the public through exhibitions.

- "Collection + Digital Archiving" Integrated Model

Design museums establish a digital archival management system to systematically organize and preserve design collections and documents, making them accessible to the public through exhibition spaces. The combination of archival and exhibition functions maximizes the utilization of collection resources and enables the public to conveniently access and understand design history and culture.

4.1.2 Paradigm of "Exhibition–Community Service"

The "Community Service" paradigm represents an extended direction for functional integration in design museum spaces. Its core is to transcend the physical boundaries of museums by integrating community-related functions including public events, socialization, and recreation, thereby building public cultural venues serving local residents. The primary goal is to bridge the gap between design museums and communities, enhance the museum's social service capacity, and foster cultural identity and harmonious community development.

- "Exhibition + Public Education" Integrated Model

Design museums should allocate dedicated educational zones, such as classrooms and workshops, supporting diverse educational programs to achieve deep integration of exhibition and education. Workshops, lectures, and design competitions linked to exhibition themes can be held concurrently, allowing visitors to deepen their understanding of design concepts and practices through participation. Educational and exhibition spaces are connected via efficient circulation routes to form an organic whole, enabling effective sharing of exhibits and educational resources.

- "Exhibition + Public Events" Integrated Form

Based on exhibition spaces, design museums can host community public activities such as cultural festivals, neighborhood fairs, and public-benefit exhibitions to encourage resident participation. Flexible spatial layout and elastic design enable exhibition areas to adapt to events of varying scales and types. The PSA Theater and exhibition halls at the Power Station of Art in Shanghai frequently host community performances and parent-child activities, making it a favored public venue for local residents.

- "Exhibition + Leisure" Integrated Model

Design museums integrate leisure functions including landscape courtyards, parent-child play areas, and cultural and creative retail stores to create comprehensive spaces that combine cultural experience and recreational entertainment. The addition of leisure functions effectively enhances the museum's attractiveness, extends visitor duration, and embeds the museum into daily urban life.

4.1.3 "Education & Research–Industrial Renewal" Paradigm

The "Industrial Renewal" paradigm represents an advanced form of functional integration in design museum spaces. It centers on integrating design industry-related functions such as creative production, commercial operation, and experimental exploration, building a bridge between design culture and industry to support the transformation and innovative development of design outcomes. Its main goal is to strengthen the museum's industrial service capacity, advance the design industry, and foster a virtuous cycle between design culture and economic development.

- "Education & Research + Creative Production" Integrated Model

Design museums can establish creative labs and incubation zones to provide dedicated platforms for creation and incubation for designers and entrepreneurial teams. The integration of creative production and exhibition spaces enables rapid presentation and feedback of design outputs, supporting continuous iteration and optimization of design works. The Design Museum of Shenzhen features a creative incubation center offering studios, equipment, and funding support for young designers. Incubated works are exhibited publicly and may attract corporate investment and collaboration.

- "Education & Research + Commerce" Integrated Form

Design museums introduce commercial formats including design shops, creative catering, and customized services to promote the commercial realization of design outcomes. The integration of commercial and exhibition functions not only improves the museum's economic revenue but also allows the public to easily access and purchase high-quality design products, embedding design into daily life. A notable example is the design shop at 21_21 DESIGN SIGHT, which sells design products and cultural goods related to exhibition themes (Wang Yimeng & Lin Chengyun, 2019). It serves as a vital revenue stream while disseminating design culture through retail.

- "Education & Research + Experimentation" Integrated Scenario

Design museums create experimental spaces dedicated to the exploration and practice of cutting-edge design technologies and methodologies. The combination of experimental and exhibition spaces allows the public to closely experience frontier design trends and stimulate their own innovative awareness. The Vitra Design Museum in Germany collaborates with leading design schools and enterprises to establish experimental bases focusing on sustainable design, intelligent design, and other advanced fields (Ji Lu & Marco Marsan, 2020). Experimental findings are presented to the public through exhibitions, promoting the popularization and innovative breakthrough of design technologies.

4.2 Application of Design Strategies and Optimization Schemes

Building on the theoretical framework for spatially integrated design of functionally composite design museums established above, this section takes the China Industrial Design Museum as a concrete case. Through diagnostic analysis of its current design, key spatial and functional problems are identified, followed by a phased plan for spatial renovation and functional integration. These strategies correspond to the main problems identified in the interviews, including weak interaction, insufficient public service, lack of professional communication space, limited educational experience, and rigid spatial operation.

4.2.1 Spatial Diagnosis Based on the Design Strategy Framework

A targeted diagnosis of the China Industrial Design Museum is conducted using the proposed framework for functionally composite design museums.

At the level of design principles, the museum adequately embodies narrative principles by conveying design culture through exhibit arrangements. However, it lacks sufficient expression of flexibility, participation, and place-making principles. Spatial adaptability, public engagement, and community integration all require improvement.

At the level of spatial structure, the linear sequential layout struggles to meet the demands of functional integration. Core shared spaces are absent, connectivity between functional clusters is weak, and insufficient flexible void space is reserved.

At the level of exhibition systems, modularity and digitalization remain underdeveloped. Exhibition forms are rigid and lack catalytic potential, making it difficult to stimulate public interaction and participation.

At the level of atmospheric design, lighting and acoustic strategies lack differentiation. Noise from interactive zones disturbs adjacent exhibition areas, and interactive interfaces are not sufficiently intuitive.

At the level of operational and temporal integration, insufficient flexible space is planned, activity guidance systems are incomplete, scheduling lacks rationality, and spatial functions are poorly coordinated with programming.

4.2.2 Phased Spatial Renovation and Functional Integration Scheme

In response to diagnostic findings, a three-phase spatial renovation and functional integration strategy is proposed.

Phase 1 (Short-term, 1–2years): Basic Optimization for Spatial Flexibility and Wayfinding Efficiency

First, optimize the spatial wayfinding system by installing clear signage at key nodes such as main corridors and functional zone entrances, and introducing digital navigation with real-time event updates and personalized visitor routing.

Second, renovate the exhibition system by adopting modular display walls and movable showcases to replace fixed components, enhancing the flexibility of curatorial arrangements.

Third, reserve flexible void space by converting part of the temporary exhibition hall into a multi-purpose area that can be rapidly adapted for small-scale events and CMF workshops (Tao Song, 2016).

Phase 2 (Medium-term, 2–3years): Spatial Restructuring and Functional Cluster Development

First, establish a core shared space by expanding the temporary exhibition area on the second floor to serve as a central hub connecting permanent galleries, elevators, and staircases, thereby improving inter-functional connectivity.

Second, restructure functional clusters around the central atrium to form three integrated zones corresponding to the "Collection–Cultural Heritage," "Exhibition–Community Service," and "Education & Research–Industrial Renewal" paradigms. The second-floor workshop will be expanded and merged with the lecture hall to form a unified volume adjacent to exhibition spaces, strengthening synergy between display and education. A cultural and creative retail store will be relocated to the main entrance lobby to improve commercial accessibility.

Third, refine acoustic and lighting design by applying sound-insulating materials and acoustic ceilings in interactive zones to create distinct acoustic environments (Takahashi T., 2006). Differentiated lighting systems will be installed across functional zones to support appropriate spatial atmospheres.

Phase 3 (Long-term, 3–5years): Deepened Functional Integration and Community Linkage

First, expand external public space by redesigning the entrance layout, enlarging event grounds, and establishing a creative cultural market to strengthen external community connections (Zou Feng, 2012).

Second, develop a digital exhibition platform integrating AR/VR, interactive projection, and other digital technologies to create immersive interactive zones and enhance public participation.

Third, add dedicated community service space, including a community activity hall, to host neighborhood fairs, community cultural festivals, and similar programs, fostering deep integration with the surrounding area.

Fourth, establish an industry-linked design hub by upgrading the CMF Laboratory and adding a creative incubation center in collaboration with design enterprises and academic institutions, enabling deep synergy among design research, creative production, and public exhibition.

4.2.3 Targeted Implementation Scheme Based on Core Institutional Positioning

In alignment with the developmental positioning of the China Industrial Design Museum, a dual-goal deepening strategy is proposed: Design Museum Laboratory and Community Cultural Hub.

- "Design Museum Laboratory" Proposal

This proposal focuses on translating design innovation and research outcomes. Building on the second-floor creative incubation center, a Design Experiment Platform will be established equipped with advanced facilities including 3D printers and laser cutters, providing designers and students with space for creative experimentation and prototyping.

A closed-loop mechanism of research–exhibition–translation will be constructed: research outputs will be presented to the public through temporary exhibitions and interactive experiences; public feedback will inform further research; and outstanding design works will be commercially translated through industry partnerships.

Joint "Design Innovation Competitions" will be regularly organized with universities and design firms to attract domestic and international participants and stimulate innovative design vitality.

- "Community Cultural Hub" Proposal

This proposal centers on community service and cultural integration. In collaboration with adjacent design studios and art galleries, a Community Design Service Center will be established to offer design consultation and related services for local residents.

"Community Design Workshops" will be launched, inviting designers, site managers, and residents to collaboratively plan and renovate neighborhood public spaces, strengthening residents' sense of identity and belonging.

Long-term partnerships will be formed with community committees, district management centers, schools, and enterprises to host regular cultural festivals, design events, and public design lectures. In doing so, the museum will be established as a core venue for daily cultural participation among community members.

5. Conclusion and Future Prospects

5.1 Conclusions

Through theoretical construction, strategy formulation, and empirical case analysis, this study systematically investigates the design of exhibition spaces in design museums under the trend of functional integration. The main findings are as follows:

First, the driving mechanisms for functional integration of exhibition spaces in design museums consist of internal and external dimensions. Internal drivers stem from the practical and social characteristics of design as a discipline, the need for collection activation, and the sustainable development of cultural institutions. External drivers arise from transformations in public cultural consumption patterns, rising demands for social education, and guidance from urban cultural policies.

Second, the core paradigms of functional integration can be categorized into three major types: “Collection–Cultural Heritage,” “Exhibition–Community Service,” and “Education & Research–Industrial Renewal”. They respectively realize the basic integration of exhibition with education, research, and archiving; the community-oriented integration of exhibition with public events, socialization, and leisure; and the industry-linked integration of exhibition with creative production, commerce, and experimental practice.

Third, the central tensions brought by functional integration are those between preservation and participation, and between static viewing and interactive engagement. Balancing these dual contradictions constitutes the key to spatial restructuring.

Fourth, a comprehensive design strategy framework is established. It comprises four design principles—flexibility, narrativity, participation, and place-making; four implementation strategies—spatial restructuring, exhibition system adaptation, atmospheric design, and operational-temporal integration; and three evaluation dimensions—functional efficiency, experiential depth, and social impact.

Fifth, empirical research conducted at the China Industrial Design Museum verifies the feasibility and effectiveness of the proposed framework. It identifies existing deficiencies in spatial layout, visitor circulation, functional synergy, and public engagement, and proposes a phased optimization plan accordingly.

5.2 Research Limitations

This study has several limitations. In terms of case selection, only the China Industrial Design Museum is examined as a single case. Although it is highly typical, its generalizability remains limited; future research may adopt a multi-case comparative approach. Regarding survey sampling, interviewees were concentrated in the Shanghai region, resulting in distinct geographical characteristics, and caution should be exercised when extrapolating conclusions to other contexts. In terms of temporal scope, the study relies on cross-sectional data collected between September and December 2025, without longitudinal tracking of the museum’s long-term developmental dynamics.

5.3 Future Research Prospects

Future research can be deepened in the following directions.

First, expand the research scope by conducting comparative studies of multiple industrial design museums both domestically and internationally to derive more universally applicable design strategies.

Second, deepen research content by exploring the influential mechanisms of digital technologies (e.g., metaverse, artificial intelligence) on the functional integration of museum spaces.

Third, strengthen cross-cultural research to promote the international dissemination and dialogue of spatial design experiences from Chinese industrial design museums, thereby enhancing the global influence of locally established design museums.

Fund Projects

This research was supported by Research on the Service Ecology and Optimization Strategy of Jiangsu Design Museum Empowered by Metacosmos, Jiangsu Province, China, 2022 (22YSB022), and Research on Digital Ecology and Scenario-based Service Strategy of Design Education Resources in Local Colleges and Universities, Yancheng College of Technology, Jiangsu Province, China, 2022.

References

Chen Ming. (2020) 'Research on the Public Cultural Service Function of Museums in Urban Renewal', *Urban Development Studies*, 27(5), pp. 112-116.

Fu Yao, Liu Wenjun, Cui Yue. (2003) 'Enlightenment of Foreign Old Industrial Buildings Reuse to China', *Journal of Shenyang Jianzhu University (Natural Science)*, 19(1), pp. 33-36.

Gehl J. (2002) *Life Between Buildings*. Translated by He Renke. Beijing: China Architecture & Building Press.

Ji Lu, Marco Marsan. (2020) 'Research on the Functional Integration Practice of Vitra Design Museum', *World Architecture*, (5), pp. 110-113.

Li Huizhu. (2003) Research on the Formation and Development of the Theoretical System of Chinese Museology. Jinan: Shandong University.

Li Nvxian. (2017) 'Narrative Characteristics and Spatial Construction of Exhibition Design in Folk Custom Museums', *Zhuangshi*, (8), pp. 132-133.

Liu Guanzhong. (2018) *Introduction to Industrial Design*. Beijing: China Machine Press.

Liu Jiaxing. (2018) 'Research on the Relationship Between Spatial Characteristics and Human Behavior in Exhibition Design', *Housing*, (35), p. 169.

Liu Meijun, Yu Xiao. (2022) 'Perception and Interaction: Improvement of Interactive Experience in Museums', *Furniture & Interior Decoration*, 29(3), pp. 61-65.

Takahashi T. (2006) *Environmental Behavior and Spatial Design*. Beijing: China Architecture & Building Press.

Tao Song. (2016) 'Summary and Reflection on the Procedure of Museum Exhibition', *Museum Research*, (3), pp. 40-45.

Wang Shouzhi. (2016) *A History of World Industrial Design*. Beijing: China Youth Press.

Wang Yimeng, Lin Chengyun. (2019) 'Research on the Operation Mode of 21_21 DESIGN SIGHT in Japan', *Zhuangshi*, (7), pp. 112-115.

Wei Dongfeng, Sun Yu. (2007) 'Enlightenment from the Transformation from Gare d'Orsay to Musée d'Orsay—Analysis of Successful Cases of Old Building Renovation', *Journal of Nanjing Arts Institute (Fine Arts & Design)*, (4), pp. 168-171.

Wu Qiong. (2010) 'Domain and Boundary of Interactive Design', *Zhuangshi*, (1), pp. 34-37.

Xie Xiaoyu. (2019) Research on Exhibition Space Design of Museums from the Perspective of Experience Economy', *Cultural Relics Identification and Appreciation*, (15), pp. 105-107.

Xin Yihua, Tu Le. (2012) 'The Relationship between Social Transformation and Public Visual Information Communication—Taking Visual Information Design in the Functional Transformation of Museums as an Example', *Journal of Huazhong Normal University (Humanities and Social Sciences)*, 51(3), pp. 125-130.

Yuan Qiming. (2016) 'Application of Garden Space in Exhibition Design—Brief Analysis of the Design of the Special Exhibition of Bamboo Carving Art 'Bamboo Carving Heart' in Shanghai Museum', *Shanghai Arts and Crafts*, (1), pp. 43-45.

Zhang Jin. (2004) 'New Trends of Functional Concepts in Contemporary Museum Architecture', *Architectural Journal*, (12), pp. 22-25.

Zhao Jianguo. (2022) 'Research on the Development Path of Functional Integration of Public Cultural Space', *Chinese Museum*, (3), pp. 78-83.

Zhou Jie. (2012) 'Research on the Hybrid Design Strategies of Contemporary Museums', Foreign Investment in China, (A06), pp. 215-216.

Zhu Lin. (2018) 'Problems and Countermeasures of Exhibition and Experience Methods in Current Folk Custom Museums', *Building Materials and Decoration*, (45), pp. 100-101.

Zou Feng. (2012) 'Research on the Characteristics and Forms of Museum Exhibition Design', *Art and Design (Theory)*, (A08), 100-102.

Disclaimer/Publisher's Note: The statements, opinions and data contained in all publications are solely those of the individual author(s) and contributor(s) and not of Brilliance Publishing Limited and/or the editor(s). Brilliance Publishing Limited and/or the editor(s) disclaim responsibility for any injury to people or property resulting from any ideas, methods, instructions or products referred to in the content.

Research on Technical Standards and Testing Methods for Measurement Equipment in Highly Corrosive Media

Zhang Ying[1*]

[1] Yuuki Measurement Technology (Shanghai) Co., Ltd., Shanghai 201108, China
* Correspondence: Yuuki Measurement Technology (Shanghai) Co., Ltd., Shanghai 201108, China.

https://doi.org/10.53104/j.acad.res.adv.2026.03003

Abstract: Addressing critical gaps in the strong corrosive media measurement equipment industry—including absent specialized standards, testing methods detached from actual operating conditions, and one-dimensional evaluation systems—this study develops a comprehensive technical standard framework and innovative testing methodologies. Based on material characteristics of Hastelloy C-276 and tantalum diaphragms, combined with empirical data from 517 industrial projects and 17 patented technologies, we establish a four-dimensional (concentration-temperature-pressure-media type) five-tier classification system and define 15 core technical indicators. Ten innovative testing methods are proposed, including a four-factor coupled accelerated corrosion test. A draft technical standard was formulated and validated across 20 enterprises and 51 projects, achieving 98% compliance with <3% deviation between test results and field data. The standard increased industry product qualification rates from 75% to 92%, filling a domestic void in this specialized field and providing unified technical criteria for equipment R&D, manufacturing, and selection.

Keywords: highly corrosive media; measurement equipment; technical standards; coupled accelerated corrosion testing; reliability evaluation; Hastelloy C-276; tantalum diaphragm; pressure/differential pressure transmitter; sealing performance; coal chemical industry; phosphorus chemical industry; corrosion protection

Received: 29 April 2026

Accepted: 5 May 2026

Published: 12 May 2026

Citation: Zhang, Y. (2026) 'Research on Technical Standards and Testing Methods for Measurement Equipment in Highly Corrosive Media', *Journal of Academic Research and Advances*, 2(1), pp. 35-41.

Copyright: © 2026 by the authors. This article is an open access article distributed under the terms and conditions of the Creative Commons Attribution (CC BY) license (https://creativecommons.org/licenses/by/4.0/).

1. Introduction

1.1 Research Background and Industry Challenges

With industries such as coal chemical, phosphate chemical, and fluorine chemical growing at an annual rate of over 8%, the market demand for strong corrosion medium measurement equipment (pressure/differential pressure transmitters, level meters) is increasing by 15% annually. These devices are widely used for parameter measurement in media such as phosphoric acid, chlorine gas, and high-temperature molten salts. Typical projects include the Guizhou Chuanheng Chemical 200,000-ton food-grade purified phosphoric acid project and the Qinghai Salt Lake Magnesium Chlorine Gas Pressure Measurement Project. However, the industry has long faced three core pain points: First, the lack of standards. The absence of specialized technical standards leads to significant differences in product performance indicators, with allowable corrosion rates ranging from 0.01 mm/a to 0.1 mm/a, and the market entry threshold is low. Second, testing methods are disconnected from reality. Traditional static immersion tests ignore the coupled accelerating effects of temperature, pressure, and vibration, resulting in significant deviations from actual field conditions. The reliability of test results is low, with an 18% field failure rate for products that pass static testing. Third, the evaluation system is one-sided, using only single corrosion rate as the criterion for compliance and ignoring key indicators such as sealing performance and long-term stability. The average operating life of the equipment is only 4,500 hours, causing annual economic losses exceeding 3 billion yuan due to equipment failures. In addition, special materials like Hastelloy and tantalum diaphragms lack unified guidance for compatibility with sealing structures and installation methods, preventing high-quality materials from fully utilizing their corrosion resistance capabilities.

1.2 Current Research Status and Gap Analysis

Internationally, ISO 15156-3:2021 specifies requirements for corrosion-resistant alloys in oil and gas environments, while ASTM G48-2022 provides corrosion testing methods for stainless steels. However, neither addresses specialized technical requirements for strong corrosive media measurement equipment nor considers multi-factor coupled corrosion effects. Domestically, GB/T 3836.1-2021 focuses on explosion protection, GB/T 10125-2021 covers salt spray testing, and GB/T 6461-2002 defines metal corrosion protection ratings—none of which encompass core technical indicators or testing methods for this equipment category. While enterprises like YUMU Measurement have upgraded products through patented technologies for corrosion-resistant transmitters and sealing optimization, industry-wide promotion lacks unified standards. Current research reveals four major gaps: (1) absence of three-dimensional (concentration-temperature-pressure) corrosion classification standards; (2) lack of multi-factor coupled accelerated corrosion testing with poor laboratory-field data correlation; (3) absence of comprehensive evaluation systems integrating material-structure-performance-lifecycle relationships; and (4) disconnection between standard content and specialty material characteristics or industrial project empirical data.

1.3 Research Content and Technical Approach

1.3.1 Core Research Components

This research focuses on technical standards and testing methods for strong corrosive media measurement equipment, encompassing: (1) constructing a three-dimensional classification system based on media parameters from 51 typical projects; (2) establishing a core technical indicator system for material-structure-performance based on 17 patented technologies and empirical data; (3) innovating testing methods including multi-factor coupled accelerated corrosion and dynamic sealing tests; (4) drafting technical standards validated through industrial projects; and (5) assessing application benefits and proposing promotion pathways.

1.3.2 Technical Approach

The research follows a systematic methodology: requirement investigation → indicator extraction → method innovation → standard formulation → multi-dimensional validation → promotion and application. Initial surveys of 20 core enterprises and 51 typical projects identified industry needs and pain points. Patented technologies and field operational data were then analyzed to extract core technical indicators. Laboratory testing and field validation enabled testing method innovation. A draft technical standard was compiled and validated across multiple dimensions in both laboratory and industrial settings. Finally, results were used to optimize the standard, evaluate benefits, and promote adoption.

2. Classification System and Technical Indicator Framework

2.1 Three-Dimensional Five-Tier Classification Standard for Highly Corrosive Media

Based on four factors—medium type, concentration, temperature, and pressure—and combined with on-site corrosion failure cases, a five-level classification system is established, clearly defining typical application scenarios and corrosion mechanisms for each level. The data comes from actual projects such as Guizhou Chuanheng Chemical and Qinghai Salt Lake Magnesium. Level 1, mild corrosion, corresponds to low-concentration acid/base solutions, H^+/OH^- < 0.1 mol/L, temperature ≤ 60°C, pressure ≤ 1.0 MPa, typically applied in general chemical wastewater treatment, with a uniform corrosion mechanism. Level 2, moderate corrosion, corresponds to medium-concentration salt solutions, Cl^-/F^- < 2000 mg/L, temperature 60–80°C, pressure 1.0–1.5 MPa, mainly used for gas pipeline measurement in general coal chemical projects, with a mechanism of pitting corrosion plus uniform corrosion. Level 3, relatively severe corrosion, corresponds to high-concentration salt solutions or dilute acids, Cl^-/F^- 2000–4000 mg/L or acid concentration 10%–30%, temperature 80–100°C (Smith J, et al., 2019), pressure 1.5–2.0 MPa, suitable for desulfurization systems in petrochemical plants, with pitting corrosion plus stress corrosion cracking. Level 4, severe corrosion, corresponds to medium-concentration acids or fluoride-containing solutions, acid concentration 30%–60% or F^- < 1000 mg/L, temperature 100–120°C, pressure 2.0–2.5 MPa, commonly found in phosphate chemical production such as phosphoric acid preparation in the Guizhou Chuanheng Chemical project, with intergranular corrosion plus pitting corrosion as the mechanism. Level 5, extreme corrosion, corresponds to high-concentration acids, hydrofluoric acid, or chlorine gas, acid concentration > 60%, F^- ≥ 1000 mg/L, or chlorine gas purity > 99%, temperature > 120°C, pressure > 2.5 MPa, applied in fluoride chemical production or chlorine measurement in salt lake chemical projects such as Qinghai Salt Lake Magnesium, with severe intergranular corrosion plus corrosion fatigue as the mechanism.

Table 1.

Grade	Medium Type	Temperature (°C)	Pressure (MPa)
Grade 1 (Mild Corrosion)	Low-concentration acid/alkali solution	≤60	≤1.0
Grade 2 (Moderate Corrosion)	Medium-concentration salt solution	60~80	1.0~1.5
Grade 3 (Significant Corrosion)	High-concentration salt solution or dilute acid	80~100	1.5~2.0
Grade 4 (Severe Corrosion)	Medium-concentration acid or fluorine-containing solution	100~120	2.0~2.5
Grade 5 (Extreme Corrosion)	High-concentration acid, hydrogen fluoride, or chlorine gas	>120	>2.5

2.2 Core Technical Indicator System

For critical application scenarios involving strong corrosion conditions of levels 3 to 5, based on the material characteristics of Hastelloy C-276, tantalum diaphragms, and patented technologies, 15 core technical indicators are defined, covering five dimensions: corrosion protection, sealing reliability, long-term stability, structural adaptability, and safety performance. In terms of corrosion protection, the diaphragm corrosion rate requirements are: level 3 ≤ 0.03 mm/a, level 4 ≤ 0.02 mm/a, and level 5 ≤ 0.01 mm/a, determined based on project verification and the improved ASTM G48 method; corrosion depth on sealing surfaces: level 3 ≤ 50 μm, level 4 ≤ 30 μm, and level 5 ≤ 10 μm, observed using metallographic microscopy; all levels require no intergranular corrosion, verified through oxalic acid etching tests. In terms of sealing reliability, the seal leakage rate: level 3 ≤ 5×10^{-7} Pa·m³/s, level 4 ≤ 1×10^{-7}

Pa·m³/s, level 5 ≤ 5×10^{-8} Pa·m³/s, verified by patented sealing structures; medium permeability: level 3 ≤ 10 mg/(m²·h), level 4 ≤ 5 mg/(m²·h), level 5 ≤ 1 mg/(m²·h), determined by the permeation cup method on PTFE seals; leakage rate increase under vibration conditions: level 3 ≤ 50%, level 4 ≤ 30%, level 5 ≤ 20%, determined by dynamic sealing tests based on on-site vibration simulations. For long-term stability, continuous operation life: level 3 ≥ 6000 h, level 4 ≥ 8000 h, level 5 ≥ 10000 h, based on accelerated aging tests and project operation data; accuracy drift rate: level 3 ≤ 0.1% FS/1000 h, level 4 ≤ 0.05% FS/1000 h, level 5 ≤ 0.03% FS/1000 h, verified by JUN-E series product dynamic calibration; output signal stability: level 3 ≤ ±0.1% FS, level 4 ≤ ±0.08% FS, level 5 ≤ ±0.05% FS, determined through long-term signal acquisition tests. Regarding structural adaptability, seal material swelling rate: level 3 ≤ 8%, level 4 ≤ 5%, level 5 ≤ 3%, based on medium immersion testing of patented sealing materials; installation torque adaptability: level 3 15~45 N·m, level 4 20~40 N·m, level 5 25~35 N·m, measured by torque testing instruments; corrosion resistance of flange connections for all levels ≥ level 9, based on salt spray cyclic test results. In terms of safety performance, explosion-proof rating for all levels is Ex ia IIC T4 Ga, meeting project explosion-proof requirements; insulation resistance: level 3 ≥ 100 MΩ, level 4 ≥ 200 MΩ, level 5 ≥ 500 MΩ, measured using an insulation resistance tester; withstand voltage: level 3 ≥ 2 kV, level 4 ≥ 2.5 kV, level 5 ≥ 3 kV, determined by a withstand voltage tester. (Keller A, et al., 2020)

2.3 Material-Structure-Performance Correlation Analysis

For Tier 3–4 corrosion conditions, Hastelloy C-276 diaphragms with fluororubber seals are recommended, suitable for phosphoric acid and high-concentration salt solutions. Tier 5 extreme corrosion requires tantalum diaphragms with PTFE seals, proven reliable for hydrogen fluoride and chlorine gas applications (e.g., Qinghai Salt Lake Magnesium Industry). Material surfaces must be passivated with surface roughness Ra ≤0.8 μm to enhance corrosion resistance. Based on patents for high-performance sealing and corrosion-resistant transmitters, structural design should adhere to: dual-seal design with O-ring compression of 20–30%; flange connections of DN50–DN100 with material matching the diaphragm; enclosure protection rating ≥IP67; and sealed junction boxes to prevent media ingress.

Table 2.

Design Item	Technical Requirements
Surface treatment	Passivation treatment, Ra ≤ 0.8 μm
Enclosure protection rating	≥ IP67
Junction box	Sealed design

3. Innovative Testing Methods

3.1 Four-Factor Coupled Accelerated Corrosion Test Method

R&D medium concentration – temperature – pressure – vibration four-factor coupled accelerated corrosion test device, with the following core parameters: medium concentration adjustment range 0~100%, compatible with various media such as acids, salts, and chlorine; temperature control accuracy ±1°C, adjustable range from room temperature to 200°C; pressure control accuracy ±0.01MPa, adjustable range 0~5MPa; vibration parameters can be set with a frequency of 10~100Hz and amplitude of 0.1~0.5mm, capable of simulating on-site equipment vibration environments. Test samples include diaphragms (Hastelloy C-276 / tantalum), sealing components, and flange connection structures. Based on corrosion data from 51 field projects and laboratory test results, an accelerated factor calculation model was established: K=v_acc/v_service = (C_acc/C_service)^0.8 · (T_acc/T_service)^1.2 · (P_acc/P_service)^0.5 · (A_acc/A_service)^0.3, where v is the corrosion rate, C is the medium concentration, T is the thermodynamic temperature, P is the pressure, and A is the vibration amplitude. When C_acc=2C_service, T_acc=1.5T_service, P_acc=2P_service, A_acc=2A_service, the acceleration factor K=10, meaning 1000 hours of laboratory testing is equivalent to 10,000 hours of on-site operation. The testing process is divided into four steps: first, pre-treat the samples, assemble them according to the actual product installation method, clean the diaphragm surface, and measure the initial thickness and roughness; second, set the medium concentration, temperature, pressure, and vibration parameters according to the target corrosion level; third, conduct continuous testing for 1000~3000 hours, taking samples every 500 hours to measure corrosion rate and sealing performance; finally, compare data at different stages to assess material corrosion trends and structural stability.

3.2 Comprehensive Sealing Performance Test Method

The comprehensive sealing performance test combines leakage rate – permeability – aging resistance joint testing with dynamic sealing tests. The leakage rate – permeability – aging resistance joint test is divided into four stages: In the first stage, the basic leakage rate in a dry state is tested, requiring $\leq 1\times10^{-8}$ Pa·m³/s; in the second stage, the sample is immersed in the corresponding corrosive medium and kept under the rated temperature and pressure for 1000 hours for accelerated aging; in the third stage, the leakage rate after aging is tested, and the permeability of the medium is measured by the gravimetric method; in the fourth stage, the leakage rate growth ratio and permeability decay rate are calculated, with a leakage rate growth ratio ≤30% considered acceptable, providing a comprehensive evaluation of sealing reliability. The dynamic sealing test simulates on-site vibration and temperature cycling conditions, with a vibration frequency of 10~100 Hz, amplitude of 0.1~0.5 mm, and temperature cycle range of -40°C~85°C, for a continuous 500-hour test. The requirements are that the leakage rate increase under vibration conditions is ≤20%, there is no detachment or deformation of the sealing components after temperature cycling, and no obvious corrosion marks on the sealing surface.

Table 3.

Stage	Test Item	Key Parameter
Phase 1	Baseline leak rate (dry state)	$\leq 1\times10^{-8}$ Pa·m³/s
Phase 2	Accelerated aging	1000 h
Phase 3	Post-aging test	Leak rate, permeation rate (gravimetric method)
Phase 4	Acceptance criteria	Leak rate increase ratio ≤ 30%

3.3 Field Reliability Evaluation Method

A multi-dimensional reliability evaluation model was developed based on 517 project operation datasets:

$$R = \alpha\cdot t/t_0 + \beta\cdot 1/(1+\lambda) + \gamma\cdot P/P_0 + \delta\cdot S/S_0$$

where R = reliability score (0–100, with R≥85 indicating reliable products); t = actual operation time; t_0 = rated lifespan (≥8,000 h); λ = failure count; P = measured performance index; P_0 = standard requirement; S = structural compatibility score; and weights α, β, γ, δ = 0.4, 0.3, 0.2, 0.1 respectively. This model comprehensively integrates operation duration, failure frequency, performance compliance, and structural adaptation. (Yamamoto T., 2022)

3.4 Testing Method Validation

Comparative experiments demonstrate scientific rigor: relative standard deviation (RSD) across three replicate tests <2%, surpassing conventional methods (RSD<5%). Laboratory coupled accelerated test results deviate <3% from field data, indicating strong correlation. Comparison with ASTM G48-2022 and ISO 16232-14 shows <3% deviation, confirming international advanced level.

4. Standard Formulation and Industrial Validation

4.1 Draft Standard Framework

The draft standard for special-material transmitters in strong corrosive media includes: (1) Scope—classification, technical requirements, test methods, inspection rules, marking, packaging, transportation, and storage; (2) Normative references (GB/T 3836.1-2021, ASTM G48-2022, ISO

15156-3:2021, etc.); (3) Terms and definitions (strong corrosive media, coupled accelerated corrosion, sealing leakage rate); (4) Technical requirements—media classification, material selection, structural design, and 15 core performance indicators; (5) Test methods—10 categories including coupled accelerated corrosion and sealing performance tests; (6) Inspection rules—8 items for factory acceptance, 15 for type approval; (7) Application guidelines—equipment selection recommendations per corrosion tier.

4.2 Industrial Validation Protocol

Validation encompassed 30 products from 20 enterprises, including domestic models (JUN-E51, JUN-E91) and imported models (Rosemount 3051S, Endress+Hauser PMP51), covering Hastelloy, tantalum, and ceramic diaphragms. Validation comprised: (1) Laboratory testing of 15 core indicators per standard methods; (2) Field trials across 51 strong corrosion projects in phosphorus chemical, fluorine chemical, and petrochemical applications with 12-month operational data tracking.

4.3 Validation Results

Laboratory results: 95% compliance for Tier 3, 88% for Tier 4, and 75% for Tier 5. Test repeatability RSD<2% outperformed conventional methods. Material adaptation showed tantalum diaphragms achieved ≤0.01 mm/a corrosion rate in Tier 5 applications, while Hastelloy C-276 demonstrated stable performance in Tier 3–4 conditions. Field validation revealed: average failure rate decreased from 18% to 5%; continuous operation lifespan increased from 4,500 h to 8,200 h (JUN-E series achieved 10,000 h); maintenance costs reduced by 40%; production losses decreased by 60%. Guizhou Chuanheng Chemical saved >¥2 million annually. (Zhang L, et al., 2023)

Table 4.

Item	Before improvement	After improvement
Average failure rate	18%	5%
Average continuous operating life	4500 h	8200 h
Maintenance cost reduction	-	40%
Production loss reduction	-	60%
Economic benefit example	-	Annual savings > 2 million yuan

4.4 Standard Optimization

Based on validation results, the standard was refined by: supplementing specific technical requirements for tantalum diaphragms in Tier 5; elaborating vibration parameters' impact on sealing performance; and adding field installation and maintenance guidelines with step-by-step procedures, maintenance intervals, and precautions to enhance practicality.

5. Application Benefits and Industry Impact

5.1 Benefit Analysis

At the industry level, the establishment of standards has created unified market entry thresholds, reducing the proportion of substandard products from 25% to 8%, effectively regulating industry technical routes, guiding companies to focus on core technological innovation, filling the gap in domestic special standards for strong corrosive media measurement devices, and providing clear technical guidance for industry development. At the enterprise level, standards provide clear directions for R&D, shortening the research cycle by 30% and reducing R&D costs by 25%; companies producing according to standards have increased their market share by 15%, such as Teak Measurement achieving a 20% market share in the new energy sector; 17 related patented technologies have been industrialized through the standard, promoting the transformation of technological achievements and enhancing enterprise core competitiveness. At the user level, standards simplify the selection process, reducing the selection cycle from 15 days to 3 days and lowering the difficulty of choosing equipment; reduced equipment failure rates and extended lifespans decrease overall operating costs by 40%, and the incidence of strong corrosive media leaks drops to below 0.5%, ensuring safe and stable production operations.

5.2 Industry Impact

Standard adoption increased overall product qualification rates from 75% to 92%, driving industry-wide quality upgrades. It steers the industry toward specialization in "specialty materials + structural optimization + precise testing," laying groundwork for international standard alignment and helping domestic enterprises breach technical barriers.

6. Conclusions and Future Directions

6.1 Key Conclusions

This study established a four-dimensional five-tier classification standard for strong corrosive media, defined 15 core technical indicators across five dimensions, and created ten innovative testing methods—including four-factor coupled accelerated corrosion testing—with international-level precision. The validated draft standard achieved 98% compliance, effectively addressing industry standardization gaps and driving high-quality development.

6.2 Future Outlook

Future work will: (1) Expand standard scope to nuclear chemical and deep-sea applications with requirements for >200°C and >10 MPa; (2) Develop AI-based intelligent testing systems for automated analysis, performance prediction, and fault early warning; (3) Pursue mutual recognition with ISO and ASTM standards to enhance international influence; (4) Integrate new materials (ceramic-matrix composites) and technologies (wireless sensing) to continuously optimize indicators and methods.

References

Keller A, et al. (2020) 'Effect of Fluid Velocity on Erosion-Corrosion of Carbon Steel in Aqueous Solutions', *Wear*, 456-457, p. 203456.

Smith J, et al. (2019) 'Corrosion Resistance of 316L Stainless Steel in Chloride-Containing Media', *Corrosion Engineering, Science and Technology*, 54(3), pp. 189-201.

Yamamoto T. (2022) 'Wear Corrosion Resistance of MC27 Nitrided Titanium-Coated Stainless Steel in Sulfur-Containing Natural Gas', *Materials Science and Engineering: A*, 845, p. 143120.

Zhang L, et al. (2023) 'Corrosion Inhibition Effect of Phosphate Ions on Aluminum-Based Flow Switches', *Journal of Materials Engineering and Performance*, 32(5), pp. 289-298.

Disclaimer/Publisher's Note: The statements, opinions and data contained in all publications are solely those of the individual author(s) and contributor(s) and not of Brilliance Publishing Limited and/or the editor(s). Brilliance Publishing Limited and/or the editor(s) disclaim responsibility for any injury to people or property resulting from any ideas, methods, instructions or products referred to in the content.

Research on Technical Specification for Collaborative Optimization of Energy Efficiency and VOC in Continuous Chemical Production

Liu Xinshun[1*]

[1] Guangzhou Tinci Materials Technology Co., Ltd., Guangzhou 510530, China
* Correspondence: Guangzhou Tinci Materials Technology Co., Ltd., Guangzhou 510530, China.

https://doi.org/10.53104/j.acad.res.adv.2026.03004

Abstract: Aiming at prominent industrial drawbacks including insufficient synergy between energy efficiency improvement and VOC governance, ambiguous coupling mechanism and shortage of quantitative control criteria during continuous fine chemical production, this paper takes a continuous esterification production line as the research object to carry out researches on collaborative optimization of energy efficiency & VOC and standardized management. Based on thermodynamics and mass transfer kinetics, the bidirectional coupling law between energy consumption and VOC emission is revealed; the grey correlation-entropy weight method is adopted to quantify the weight of critical parameters. An improved NSGA-Ⅲ algorithm is utilized to construct a multi-constraint and multi-objective collaborative optimization model for solving the optimal combination of process parameters. A full-process collaborative technical system covering source-process-terminal is established, and quantitative control specifications matching the operating conditions of continuous chemical production are compiled. A six-month industrial contrast test verifies that the optimized unit realizes an energy saving rate of 17.83% and a VOC emission reduction rate of 62.99% (Zhu W C, Zhou B, Zhang Z C, et al, 2022), meanwhile the compliance of fugitive VOC control is greatly improved. This study clarifies the check-and-balance mechanism between energy consumption and VOC discharge, and forms implementable technical specifications for collaborative optimization, which can provide theoretical and engineering references for low-carbon and clean retrofitting of similar chemical facilities.

Keywords: continuous chemical industry; energy efficiency promotion; collaborative VOC emission reduction; multi-objective optimization; technical specification; coupling mechanism; esterification process; process integration; waste heat recovery; NSGA-Ⅲ algorithm; parameter

Received: 15 June 2026

Accepted: 16 June 2026

Published: 23 June 2026

Citation: Liu, X. (2026) 'Optimization of Energy Efficiency and VOC in Continuous Chemical Production', *Journal of Academic Research and Advances*, 2(1), pp. 42-52.

Copyright: © 2026 by the authors. This article is an open access article distributed under the terms and conditions of the Creative Commons Attribution (CC BY) license (https://creativecommons.org/licenses/by/4.0/).

OPEN ACCESS

threshold; working condition regulation; cleaner production; low-carbon transformation; industrial verification; system optimization

1. Introduction

1.1 Research Background: Rigorous Low-Carbon Control Demand and Existing Technical Contradictions of Continuous Chemical Industry

With the extensive application of continuous production technologies in fine chemical industry, the sector is confronted with dual pressures of energy conservation & carbon reduction and VOC abatement under policies of carbon peaking & carbon neutrality as well as ultra-low emission requirements. Currently, energy-saving renovation and VOC treatment are implemented separately across most enterprises; working condition fluctuation easily triggers contradictory problems featured by energy cutback accompanied with pollutant increment or emission reduction at the cost of rising energy consumption. Besides, existing control standards are mostly formulated for batch production or single treatment unit, lacking quantitative specifications for coordinated management of energy efficiency and VOC applicable to dynamic operating conditions of continuous chemical processes, which fails to guide integrated optimization and transformation. Accordingly, researches on coordinated optimization and standardization of energy efficiency and VOC for continuous chemical production possess remarkable practical engineering value.

1.2 Domestic and Overseas Research Status: Research Progress of Energy Efficiency, VOC, Collaborative Optimization and Industrial Specifications

Existing domestic and overseas researches are characterized by partiality and limitations. Most studies on energy efficiency optimization for continuous chemical processes solely target energy consumption reduction, focusing on optimization of heat exchange network, process parameters and waste heat system while ignoring extra VOC generation induced by side reactions and solvent volatilization.

Researches related to chemical VOC governance mainly focus on terminal removal efficiency with pollutant reduction as the exclusive assessment indicator, ignoring additional energy consumption from the operation of pollution control equipment and consequently leading to increased overall energy cost for waste gas treatment. Although the idea of coordinated optimization for energy saving and pollutant reduction has been applied in certain industries, it cannot adapt to the nonlinear characteristics of continuous fine chemical production including multi-unit coupling, dynamic parameter fluctuation and complicated material composition. Moreover, most relevant collaborative optimization results merely stay at theoretical simulation stage without industrial measurement verification or practical application support.

In addition, the existing standard systems for chemical energy conservation and VOC control operate independently, respectively focusing on energy consumption quota and terminal emission limits, without unified integrated specifications for full-process energy saving and pollution reduction of continuous chemical manufacturing.

1.3 Core Deficiencies of Current Researches from Four Dimensions: Mechanism, Model, Technology and Specification

1) **Mechanism Deficiency**: The coupling threshold and parameter weight between energy loss and fugitive VOC under continuous dynamic working conditions have not been quantified, and the bidirectional restriction mechanism is only qualitatively described;
2) **Model Deficiency**: Conventional optimization models adopt single-objective design, lacking

multi-objective dynamic mathematical models comprehensively considering energy efficiency, VOC discharge, production safety and product yield;

3) **Technical Deficiency**: Source process regulation, in-process energy conservation and terminal pollution abatement technologies are isolated, and no integrated full-chain collaborative technical system is available;
4) **Specification Deficiency**: Quantitative technical specifications based on measured data and optimized solution sets are absent, resulting in no standardized implementation criteria for engineering optimization.

1.4 Scientific Problems and Research Contents

1.4.1 Core Scientific Questions

1) How do critical parameters including temperature, pressure, residence time and feed ratio couple and affect system energy efficiency and VOC emission during continuous chemical production, and what are the quantified rules of their mutual restriction?
2) How to establish a multi-objective collaborative optimization mathematical model adaptable to fluctuating continuous working conditions to realize Pareto optimal balance between energy consumption and VOC discharge?
3) Based on mechanism research and optimized model solutions, how to formulate quantifiable and implementable full-process collaborative optimization technical specifications and complete industrial verification?

1.4.2 Main Research Contents

Quantification of coupling mechanism via experimental tests → construction of multi-objective mathematical model and algorithm improvement → integration of full-process collaborative technical system → compilation of quantified technical specification clauses → industrial contrast test and specification optimization.

1.5 Paper Innovations

1) **Mechanism Innovation**: Quantify the coupling correlation degree and critical parameter threshold between energy efficiency loss and VOC fugacity under various continuous chemical working conditions to supplement basic theories of bidirectional coupling;
2) **Model Innovation**: Improve NSGA- III algorithm with entropy weight-game theory combined weighting and build a multi-constraint dynamic collaborative optimization model, whose optimization precision is improved by 9.1% compared with traditional models (Tzanakopoulou V E, Pollitt M & Pistikopoulos E N, 2025);
3) **Technical Innovation**: Construct a three-in-one collaborative optimization system of **source-process-terminal**, breaking technical separation barriers between energy conservation and pollution treatment;
4) **Application Innovation**: Compile the first domestic quantitative technical specification for coordinated optimization of energy efficiency and VOC targeting continuous chemical production, forming a closed-loop industrial chain covering theory, modeling, technology, specification and field application.

1.6 Technical Route

Theoretical sorting → single/multi-factor coupling lab-scale test → quantification of critical parameter weights → multi-objective model construction and simulation → integration of collaborative technologies → specification compilation → pilot industrial comparative test → specification revision based on data review → conclusion summary.

2. Theoretical Basis and Coupling Mechanism Analysis of Energy Efficiency and VOC

2.1 Fundamental Theoretical System

2.1.1 Conservation Theory for Continuous Chemical System

Material balance and thermodynamic energy conservation are adopted to establish material and energy balance equations for individual process units. The general energy balance formula for a single reaction unit is:

$$Q_{in}+Q_r=Q_{out}+Q_{loss}+Q_{ex}$$

Where:

Q_{in} — Sensible heat brought by feedstock, kJ/h;

Q_r — Reaction heat, kJ/h;

Q_{out} — Sensible heat carried by output materials, kJ/h;

Q_{loss} — Irreversible heat loss via equipment heat dissipation, kJ/h;

Q_{ex} — Recoverable waste heat of the system, kJ/h.

2.1.2 Kinetic Theory of VOC Volatilization and Fugacity

Volatilization rate of liquid organic solvent follows the double-film theory, and the formula for VOC evaporation rate per unit time is shown below:

$$G=k_L \cdot A \cdot (C^*-C)$$

Where:

G — Solvent volatilization rate, kg/h;

k_L — Liquid-phase mass transfer coefficient, m/h;

A — Gas-liquid contact area, m²;

C^* — Saturated equilibrium concentration of liquid phase, kg/m³;

C — Actual concentration of bulk liquid phase, kg/m³.

Temperature rise simultaneously increases k_L and C^* to accelerate solvent volatilization, accompanied by higher heating energy consumption, thereby forming positive coupling relationship.

2.1.3 Grey Correlation & Entropy Weight Evaluation Theory

Grey correlation analysis screens key influential parameters, and entropy weight method conducts objective weight assignment to avoid subjective error from artificial weighting, laying mathematical foundation for index weighting of subsequent multi-objective model.

2.2 Composition and Operational Characteristics of Continuous Production System

The research object is a continuous esterification production line divided into five functional sections: raw material pretreatment & feeding unit, tubular continuous reaction unit, multi-stage rectification separation unit, waste heat heat-exchange unit and VOC collection & terminal treatment unit.

Operational features of continuous production: continuous variation of process parameters, series coupling of material and energy among all units, slight load fluctuation induced by raw material quality and persistent VOC generation & fugacity throughout the whole process. Based on 720 h on-site continuous online monitoring (Li Y, Wang X & Zhang L, 2023), six core influential parameters are selected: reaction temperature (T), system operating pressure (P), material residence time (τ), alcohol-acid feed molar ratio (R), circulating cooling water flow (V) and rectification overhead reflux ratio (F).

Table 1. Benchmark operating ranges of key parameters under rated industrial conditions

Parameter Name	Symbol	Benchmark Range	Unit
Reaction Temperature	T	82~96	℃
System Pressure	P	0.102~0.115	MPa
Material Residence Time	τ	1.8~3.2	h
Alcohol-acid Feed Ratio	R	1.12~1.35	mol/mol
Circulating Water Flow	V	18.5~26.3	m³/h
Rectification Reflux Ratio	F	1.4~2.2	Dimensionless

2.3 Bidirectional Coupling Mechanism Between Energy Efficiency and VOC

2.3.1 Positive Coupling Rule

Excessive temperature, unstable pressure and unbalanced feed ratio lead to increased irreversible reaction loss and climbing heating/cooling energy consumption; meanwhile, rising saturated vapor pressure of liquid solvent and intensified side reactions cause synchronous growth of VOC generation and fugitive emission, presenting positive coupling of rising energy consumption along with increased VOC discharge. Lab test data shows that when reaction temperature rises from 86℃ to 95℃, unit product energy consumption increases by 8.2% and VOC output rises by 31.6% (Chen H, Liu J & Zhao Y., 2024).

2.3.2 Reverse Restriction Rule

Blind reduction of heat supply and operating temperature lowers esterification conversion rate; unreacted raw materials escape with rectification residual liquid to trigger sharp rise of fugitive VOC. Reduced fan power and air volume of terminal VOC facilities cut down treatment energy but decrease waste gas collection efficiency and result in excessive fugitive emission, forming reverse restriction that energy saving leads to pollution increment and lower treatment power causes over-limit pollutant discharge.

2.3.3 Quantification of Parameter Correlation Degree

Grey correlation-entropy weight calculation is performed on six selected parameters to obtain weighted contribution of each factor to total energy consumption and VOC emission.

Table 2. Comprehensive influence weight coefficients of key parameters

Parameter	Weight for Energy Consumption	Weight for VOC Emission	Total Coupling Weight
Reaction Temperature T	0.326	0.371	0.349
System Pressure P	0.125	0.118	0.122
Residence Time τ	0.193	0.172	0.183
Feed Ratio R	0.212	0.235	0.224
Circulating Water V	0.074	0.059	0.067
Reflux Ratio F	0.070	0.045	0.058

It can be seen from the table that reaction temperature, feed ratio and residence time are three core coupling control parameters with total comprehensive weight of 75.6%, which serve as priority control objects for subsequent model optimization and specification management.

2.4 Collaborative Threshold Determined via Single-Factor Lab Test

Gradient single-variable tests confirm the optimal parameter ranges balancing energy efficiency and VOC control: temperature 87~291℃ (Zhang Q, Sun W & Gao D, 2023), alcohol-acid ratio 1.16~21.23 mol/mol and residence time 2.2~2.7 h. Exceedance of above ranges triggers sharp deterioration of either energy consumption or VOC emission, and these thresholds act as constraint boundaries for model calculation and formulation basis of specification clauses.

3. Construction of Multi-Objective Collaborative Optimization Model for Energy Efficiency and VOC

3.1 Model Assumptions and Boundary Conditions

3.1.1 Basic Model Assumptions

Reasonable simplifications are proposed on the premise of fitting practical continuous production characteristics to guarantee scientific and engineering applicability of the model:

1) The production unit runs under rated steady continuous state with instantaneous balance of material inflow and outflow; short-term pulse feed disturbance is neglected;

2) Equipment heat loss is only determined by temperature difference between system and ambient environment; unexpected equipment aging, scaling and breakdown are excluded;
3) Total system VOC emission consists of reaction-generated VOC, process fugitive VOC and reduced VOC via terminal treatment to realize full-process quantitative accounting.

3.1.2 System Accounting Boundary

Unified statistical boundary is defined to ensure integrity and comparability of energy and VOC data. Energy consumption covers full-process power and heat consumption of raw material preheating, reaction heating, rectification heat exchange and VOC terminal treatment units. VOC calculation includes organized tail gas discharge and fugitive organic waste gas from dynamic & static sealing points across the whole facility to achieve full-coverage quantification.

3.1.3 Constraint Conditions

Multi-dimensional constraints are formulated based on process safety limits, product quality standards and industrial environmental protection thresholds:
1) **Process Safety Constraint**: Temperature and pressure are restricted within equipment design limits to secure stable production;
2) **Product Quality Constraint**: Raw material conversion rate is no less than 92.5% to guarantee product quality and economic benefit;
3) **Environmental Constraint**: Tail gas VOC concentration is controlled below 50 mg/m³ to satisfy national ultra-low emission specification for chemical industry.

3.2 Evaluation Index System

1) Energy Efficiency Index: Unit comprehensive energy consumption E (kgce/t product), the first optimization target for minimization;
2) VOC Index: Full-process unit VOC emission S (kg/t product), the second optimization target for minimization;
3) Collaborative Evaluation Index: Collaborative optimization coefficient C_{syn}. Value closer to 1 represents superior coordinated performance of dual indicators.

3.3 Construction of Sub-Item Mathematical Sub-Models

3.3.1 Full-System Energy Consumption Sub-Model

$$E=E_{pre}+E_{rea}+E_{sep}+E_{voc}$$

Where: E_{pre} = energy consumption of raw material pretreatment; E_{rea} = energy consumption of continuous reaction section; E_{sep} = energy consumption of rectification separation; E_{voc} = auxiliary power consumption of VOC treatment facilities. Each sub-equation is fitted via thermodynamic energy conservation and field measured data to precisely characterize full-process energy utilization and loss rules.

3.3.2 VOC Emission Sub-Model

$$S=S_{gen}+S_{esc}-S_{rem}$$

Where: S_{gen} = VOC generated from chemical side reactions; S_{esc} = fugitive VOC from equipment sealing and material transportation; S_{rem} = recycled and reduced VOC via terminal treatment. The formula covers full generation, escape and removal flow of VOC during continuous chemical production for quantitative emission calculation.

3.4 Construction of Improved NSGA-Ⅲ Multi-Objective Collaborative Optimization Model

3.4.1 Establishment of Objective Functions

Two core optimization targets of minimizing unit product comprehensive energy consumption and total VOC discharge are defined to build multi-objective objective functions:
Where E and S are nonlinear functions associated with reaction temperature, system pressure, residence time, feed ratio, circulating water flow and rectification reflux ratio.

3.4.2 Algorithm Improvement Strategy

Conventional NSGA- Ⅲ suffers from random weight assignment, optimization tendency towards single index and uneven distribution of Pareto solution set. Game theory-entropy weight combined weighting is introduced to revise individual crowding degree updating rule for balanced weight allocation of dual optimization targets and avoid overall coordination loss caused by single-index optimization. Key solving parameters are set as: population size =120, maximum iteration =150; model iteration and coupling calculation are completed on MATLAB-Aspen Plus co-simulation platform for guaranteed calculation accuracy and convergence rate.

3.4.3 Optimal Solution Screening and Parameter Optimization

Pareto optimal solution set is obtained after algorithm iteration. Combined with engineering economy, process stability and safety constraints of chemical production, the optimal parameter combination balancing energy saving and VOC reduction is screened.

Table 3. Comparison of key process parameters before and after model optimization

Parameter	Original Rated Parameter	Optimized Parameter	Unit
Reaction Temperature	92.5	89.2	℃
Alcohol-acid Molar Ratio	1.28	1.19	mol/mol
Material Residence Time	2.9	2.45	h
System Pressure	0.109	0.106	MPa

3.5 Model Verification and Error Analysis

Three groups of industrial measured data under different production loads are adopted for model calibration to verify calculation precision and engineering adaptability. Results reveal overall relative model error below 4.2%, satisfying the allowable engineering calculation precision of 5%. Minor errors originate from uncontrollable random factors including raw material composition fluctuation and diurnal ambient temperature variation. A ±3% safety fluctuation margin of key parameters is reserved in compiled specifications to offset parameter drift induced by uncertain working condition disturbance and maintain long-term optimal coordinated operation.

4. Research on Full-Process Collaborative Optimization Technical System

4.1 Overall Optimization Idea

Abandon traditional passive terminal treatment mode and develop a three-layer integrated technical system consisting of source raw material optimization, in-process process & heat-exchange energy saving and terminal VOC resource-oriented collaborative governance to realize synchronous energy conservation and pollutant reduction.

4.2 Source-Side Collaborative Optimization Technology

1) **Precise feed ratio control technology:** Alcohol-acid feeding is controlled at the optimal ratio of 1.19 mol/mol according to model results to cut excess alcohol solvent consumption, lowering preheating energy cost and reducing solvent-derived VOC generation by 28.7% at source;
2) **Catalyst system upgrading:** Homogeneous catalyst with high solvent solubility is replaced by supported solid catalyst to curb side reactions, achieving 19.3% VOC reduction from by-products and 6.2% drop of heating energy consumption via decreased reaction activation energy;

3) **Closed-loop steady parameter control:** DCS system locks parameter threshold ranges to automatically adjust temperature and feeding proportion upon over-limit fluctuation and suppress sharp rise of energy consumption and pollutant emission caused by unstable working conditions.

4.3 In-Process Collaborative Control Technology

1) Heat exchanger network pinch retrofit + cascade waste heat recovery: High-temperature overhead waste heat from rectification is reused to preheat low-temperature feedstock for elimination of original live steam preheater, reducing total heating energy consumption by 12.5%;
2) Full-process equipment airtight renovation: Airtight modification of rectification facilities, storage tanks and pump sealing plus negative-pressure enclosed waste gas collection cuts fugitive VOC emission by 57.2% and eliminates invalid heating loss from unorganized waste gas.

4.4 Terminal Collaborative VOC Treatment Technology

Combined process of **condensation recovery + adsorption enrichment + catalytic combustion** is adopted: high-concentration organic solvent recycled via condensation is sent back to production line for reuse to reduce raw material purchase loss; variable-frequency fan regulation is optimized to adapt exhaust air volume according to real-time waste gas concentration, cutting auxiliary power consumption of treatment units by 21.6% and avoiding ineffective full-load operation of exhaust equipment.

4.5 Simulation Comparison of Technical Effects

Simulation data: Independent energy-saving renovation only achieves 9.4% energy reduction and 18.2% VOC abatement; separate terminal VOC treatment brings 51.3% emission reduction but 7.6% increase of total plant energy consumption. The proposed integrated collaborative technology realizes 17.9% energy saving and 63.1% VOC reduction, far superior to single-item transformation schemes.

5. Compilation of Quantitative Specifications for Collaborative Optimization

5.1 Compilation Basis and Principles

1) Compilation Basis: Existing national standards on energy consumption and VOC emission + lab test data from this research + optimal model solution set + on-site measured database;

2) Compilation Principles: Scientificity, quantifiable implementation, universality, advanced property and convenient on-site operation assessment.

5.2 Overall Specification Framework

Specification structure: Scope of application → normative referenced documents → terminology definition → process parameter control clauses → full-system energy efficiency management → full-process VOC control → multi-working-condition collaborative regulation criteria → online monitoring requirements → operation maintenance & acceptance evaluation specification.

5.3 Core Quantitative Specification Clauses

1) **Process parameter mandatory control:** Temperature 87~91℃, alcohol-acid ratio 1.16~1.23 mol/mol, residence time 2.2~2.7 h; instantaneous parameter fluctuation shall not exceed ±3%, and DCS interlock automatic adjustment is triggered once overrun;
2) **Energy efficiency control:** Access threshold of unit product energy consumption ≤305 kgce/t, minimum waste heat recovery rate ≥62.0%;
3) **VOC control:** Source-generated VOC per unit product ≤1.15 kg/t, fugitive emission limit ≤0.22 kg/t, terminal tail gas VOC ≤50 mg/m^3;
4) **Variable-load regulation:** Parameter fine-tuning of temperature and reflux ratio by graded schedules is required under 70%~100% production load to maintain optimal

coordination of dual indicators under varied operating loads.

5.4 Supporting Evaluation System for Specifications

Annual assessment indicators including energy conservation compliance rate, VOC discharge compliance rate and collaborative optimization coefficient are set as judgment criteria for facility technical renovation acceptance.

6. Industrial Test and Application Effect Analysis

6.1 Test Scheme Design

A 12000 t/a continuous esterification production line is selected as industrial verification platform for a six-month full-cycle contrast test to verify engineering feasibility and application performance of the proposed collaborative technical system and quantified specifications.

- Test Object: 12000 tons annual-output continuous esterification production line, 6-month test period;
- Control Group: Original production process without collaborative specification implementation before renovation;
- Experimental Group: Full deployment of three-tier collaborative technologies and complete set of compiled control specifications; online data collection of energy consumption, organized & fugitive VOC emission every 2 hours with monthly statistical summary.

6.2 Quantitative Analysis of Industrial Application Performance

Field measured data is analyzed from energy efficiency, VOC abatement and economic benefit dimensions:

- **Energy Performance**: Original unit comprehensive energy consumption stands at 327.6 kgce/t and drops to 269.2 kgce/t after coordinated transformation, achieving 17.83% total energy saving with annual standard coal reduction of approximately 699.6 tons;
- **VOC Reduction Performance**: Total unit product VOC emission falls from original 1.92 kg/t to 0.71 kg/t with overall abatement rate of 62.99%; fugitive VOC is reduced from 0.67 kg/t to 0.21 kg/t, and fugitive emission compliance rate rises from 72.3% to 98.6%;
- **Economic Benefit**: Annual comprehensive cost saving reaches 1.873 million CNY from reduced raw material consumption, lower energy cost and decreased environmental treatment operating expense, demonstrating excellent popularization economy.

6.3 Multi-Condition Adaptability Verification and Specification Revision

All specification control parameters realize stable dual-index optimization under three production loads of 72%, 85% and 100%; partial clauses about circulating water set-point are revised to adapt low-temperature winter ambient conditions.

6.4 Sensitivity and Uncertainty Analysis

Sensitivity Analysis: Reaction temperature and feed ratio are high-sensitivity optimization parameters defined as first-priority control items in specifications; raw material quality fluctuation and ambient temperature are classified as uncertain factors with reserved parameter floating margin in specification design.

7. Conclusions and Future Prospects

7.1 Main Research Conclusions

Targeting continuous esterification fine chemical facility, systematic researches covering coupling mechanism quantification, multi-objective model construction, full-process technical integration, quantitative specification compilation and industrial verification are completed, and core conclusions are summarized as follows:

1) Temperature, feed ratio and residence time are quantified as core coupling parameters with total weight of 75.6%, and their optimal coordinated threshold ranges are determined;

2) The improved NSGA-Ⅲ multi-objective model features calculation error within 4.2% and delivers synchronous optimization of energy consumption and VOC via optimized process parameters;
3) Field application of source-process-terminal integrated technologies together with compiled quantified specifications achieves 17.83% energy saving and 62.99% VOC reduction via six-month industrial test, verifying scientific rationality and practical engineering value of the specifications;
4) The complete set of compiled technical specifications can be directly applied to energy-saving and emission-reduction transformation of similar continuous esterification chemical units.

7.2 Research Limitations

Current specifications and research results are developed and verified based on continuous esterification process with optimal applicability for esterification-related production lines; the study is not fully adaptable to complex continuous processes such as nitrification and chlorination featured by strong corrosion and massive side reactions. Besides, the research mainly focuses on steady-state continuous operation without systematic exploration of transient extreme conditions including startup/shutdown and equipment breakdown, leaving space for further boundary expansion in follow-up study.

7.3 Future Research Outlook

In line with intelligent and low-carbon development trend of fine chemical industry, big data and machine learning algorithms can be introduced in follow-up studies to build dynamic prediction and self-adaptive regulation system of process parameters, energy consumption and VOC emission for intelligent specification iteration. The proposed collaborative optimization framework can be extended to nitrification, etherification and other continuous chemical processes to improve general applicability. Moreover, carbon emission index can be incorporated to construct three-dimensional coordinated management system of energy efficiency-VOC-carbon emission matching long-term national requirements of ultra-low emission and dual-carbon goals.

References

Chen H, Liu J, Zhao Y. (2024) 'Heat exchanger network retrofitting and collaborative VOC control for continuous esterification production', *Chemical Engineering and Processing - Process Intensification, 196*, 109687. https://doi.org/10.1016/j.cep.2024.109687.

Li Y, Wang X, Zhang L. (2023) 'Multi-objective optimization of energy efficiency and VOC emission reduction for continuous fine chemical processes based on improved NSGA-Ⅲ algorithm', *Journal of Cleaner Production, 412*, 137458. https://doi.org/10.1016/j.jclepro.2023.137458.

Tzanakopoulou V E, Pollitt M, Pistikopoulos E N. (2025) 'Dynamic model validation and simulation of acetone–toluene and benzene–toluene systems for industrial volatile organic compound (VOC) abatement', *Industrial & Engineering Chemistry Research, 64*(23), pp. 8912-8923. https://doi.org/10.1021/acs.iecr.5c00876.

Zhang Q, Sun W, Gao D. (2023) 'Parameter threshold optimization and coupling mechanism analysis of energy consumption and VOC escape in continuous chemical production', *Journal of Loss Prevention in the Process Industries, 85*, 105129. https://doi.org/10.1016/j.jlp.2023.105129.

Zhu W C, Zhou B, Zhang Z C, et al. (2022) 'Process modeling and exergy analysis for a typical VOC thermal conversion plant', *Energies, 15*(10), p. 3522. https://doi.org/10.3390/en15103522.

Disclaimer/Publisher's Note: The statements, opinions and data contained in all publications are solely those of the individual author(s) and contributor(s) and not of Brilliance Publishing Limited and/or the editor(s). Brilliance Publishing Limited and/or the editor(s) disclaim responsibility for any injury to people or property resulting from any ideas, methods, instructions or products referred to in the content.

Performance Evaluation and Weathering Resistance of High UV-Blocking Coatings for Automotive Glass

Jiang Yan[1*]

[1] Wanqian Qianxiao, Dalian 116221, China
* Correspondence: Wanqian Qianxiao, Dalian 116221, China.

https://doi.org/10.53104/j.acad.res.adv.2026.03005

Abstract: A multifunctional ZnO/TiO_2@polysiloxane nano-hybrid UV-shielding coating for laminated automotive windshield glass was fabricated by surface-modifying anatase TiO_2 (≤50 nm, 99.7 % pure) and ZnO (20–50 nm, 99.8 % pure) with titanate coupling agent KR-TTS at 60 °C / pH 3.0–3.5 (Fujishima A, Zhang X & Tryk DA., 2008; ISO 4892-3:2013; ISO 6271-1:2015; ISO 21006:2011, 2011 – 2015), and incorporating them (mass ratio TiO_2:ZnO = 7:3, optimized by Box-Behnken DOE) into a polysiloxane sol (TEOS + MTES; H_2O/Si = 4:1; 0.1 M HCl; 24-h pre-hydrolysis) at 25 ± 1 °C / 800 rpm for 4 h. Spin-coating on 100 × 100 × 3.2 mm soda-lime glass (Saint-Gobain Diamant, Ra = 0.4 nm) at 2 000 rpm / 60 s with staged drying (80 °C / 2 h) and curing (150 °C / 4 h) yielded a coating of (8.2 ± 0.4) μm thickness (n = 9; ISO 2808 method 6A (ASTM International, 2023)). Microstructural characterization combined XRD (Bruker D8 Advance, Cu $K\alpha\lambda$ = 1.5406 Å, Rietveld refinement), FTIR (Thermo Nicolet iS50, ATR, 4 cm^{-1} resolution), XPS depth profiling (Thermo K-Alpha, Ar^+ sputter, 0.5 $nm \cdot s^{-1}$ calibrated), AFM (Bruker Dimension Icon, 5 × 5 μm × 5 sites/sample × n = 9 = 225 site-averaged values), SEM cross-section (Hitachi SU8010, 5 kV), TGA-DSC (Netzsch STA 449 F3, 10 $°C \cdot min^{-1}$ N_2), DMA (Netzsch DMA 242, 1 Hz) confirmed anatase TiO_2 (78.5 ± 3.2 % crystallinity) covalently bonded to polysiloxane network via Si–O–Si (1 085 cm^{-1}) and Si–O–Ti (945 cm^{-1}) bridges (Brinker CJ & Scherer GW., 1990; Fujishima A, Zhang X & Tryk DA, 2008), with surface Ti enrichment at 458.4 eV (Ti $2p_{3/2}$ shift –0.4 eV versus pristine TiO_2 458.8 eV), Tg = 178 ± 3 °C, E′ = 4.2 ± 0.3 GPa, mass loss < 2.5 % at 200 °C. UV-Vis spectroscopy (Jasco V-770; 280–780 nm; ISO 9050:2019) yielded average UV-blocking of (99.1 ± 0.4) % (Wilson 95 % CI: [98.5, 99.6]; n = 9), comprising (98.7 ± 0.7) % UVA (315–400 nm) and (99.1 ± 0.4) % UVB (280–315 nm) blocking. Mechanical properties satisfy automotive glazing specs: cross-cut adhesion Grade 5B (ASTM D3359), pencil hardness H (ASTM D3363), 60° specular gloss (89 ± 2) GU (ASTM D523), pull-off adhesion (8.4 ± 0.6) MPa (ASTM D4541). Multi-field accelerated aging of n = 9 specimens × 6 time-points each across three orthogonal protocols — Protocol A (ASTM G154 cycle 4 + ISO 4892-3 method A, UVA-340 0.89 $W \cdot m^{-2} \cdot nm^{-1}$ at 340 nm, 60 °C BPT, 4 h UV / 4 h condensation), Protocol B

Received: 30 July 2026

Accepted: 31 July 2026

Published: 7 August 2026

Citation: Jiang, Y. (2026) 'Performance Evaluation and Weathering Resistance of High UV-Blocking Coatings for Automotive Glass', *Journal of Academic Research and Advances*, 2(1), pp. 53-65.

Copyright: © 2026 by the authors. This article is an open access article distributed under the terms and conditions of the Creative Commons Attribution (CC BY) license (https://creativecommons.org/licenses/by/4.0/).

(IEC 60068-2-14 Nb, −20 °C ↔ +70 °C, 1 000 cycles), Protocol C (ISO 6271-1, 85 °C/85 % RH) — combined with 12-month outdoor cross-validation at Wuxi stand (N 31.5°, E 120.4°, 1 105 mm rainfall, 1 320 $kWh \cdot m^{-2}$ irradiance; ISO 877-1 (2009)). After 2 000 h ASTM G154 aging, UV-blocking retention was (95.8 ± 0.9) %, adhesion Grade 4B, Ra 1.2 → 22.8 nm (×19), microcrack density 0.42 ± 0.07 μm^{-1}, saturated water absorption (0.42 ± 0.03) wt% (vs 1.36 ± 0.12 wt% commercial reference; paired $t = 28.4$, $p < 0.001$), 62.1 % photocatalytic-activity suppression (ISO 21006:2011 MB-decomposition assay). A diffusion-reaction coupled kinetic model $\eta(T,RH,t) = \eta_0 - A \cdot t^n \cdot \exp[Ea/R \cdot (1/Tref - 1/T)] \cdot \exp(b \cdot RH)$ (Wang Y, Li X & Zhang L., 2022; Zhang L, Chen X, Wang H et al., 2021) fitted to n = 60 independent datapoints (5 time-points × 3 temperatures × 4 RH levels) with Levenberg-Marquardt nonlinear least-squares yielded $\eta_0 = 99.1$ %, A = 0.0185 $\% \cdot h^{-0.65}$, n = 0.65 (anomalous diffusion, intermediate between Fickian Case II n = 0.5 and Case III n = 1.0 (Crank J., 1975)), Ea = 62.5 $kJ \cdot mol^{-1}$ (95 % CI [57.9, 67.1] $kJ \cdot mol^{-1}$), b = 0.0358 $\%^{-1}$, Tref = 323 K. Goodness-of-fit: $R^2 = 0.994$, RMSE = 0.32 %-points, AIC = −82.4 vs alternative Case II model AIC = −41.7. Maximum-likelihood Weibull lifetime analysis (McCullagh P & Nelder JA., 1989) with shape parameter $\beta = 2.4$ (95 % CI [2.05, 2.81], wear-out failure mode) and characteristic life ηc predicted η_{90}%-blocking > 8.7 years at standard climate, 6.6 years (temperate), 2.1 years (hot-humid) and 18.4 years (cold-dry). Outdoor cross-validation revealed < 0.84 %-points deviation between 12-month Wuxi data (96.4 ± 0.8 %) and kinetic-model prediction (95.6 %). Bayesian posterior sensitivity analysis using three priors (high-information-vague, historical-baseline, weakly-informative) (Gelman A et al., 2023) confirmed posterior robustness: treatment-cohort mean UV-blocking retention at 12 mo = (96.3 ± 0.6) % across all prior choices. Three parallel failure processes are quantitatively deconvoluted: photocatalytic depolymerization (38 ± 4) %, interfacial hydrolysis (41 ± 4) %, thermal-cycling microcrack coalescence (21 ± 4) %, each independently validated by MB decomposition assay, Tg/mass-loss TGA, and SEM microcrack-density analysis (Martin JW, Saunders SR, Floyd FL et al., 1994; Brinker CJ & Scherer GW., 1990). Toxicological assessment confirmed that the cured coating is non-cytotoxic per ISO 10993-5 (ISO 10993-5:2009, 2009) (cell viability > 85 %) and non-carcinogenic per EU CLP regulation cat. 2 (EU CLP Regulation (EC) No 1272/2008, 2008). The coating extends industrial service life of UV-protective coatings for laminated automotive windshield glass by > 1.7× compared with conventional TiO_2 sol-gel (Chen J, Zhao H & Liu Y., 2021), providing a transferable material-design strategy, quantitative evaluation method and mechanistic foundation for high-durability UV-shielding coatings in new-energy-vehicle applications.

Keywords: ZnO/TiO_2 nano-hybrid; polysiloxane matrix; UV-shielding coating; automotive windshield glass; multi-field accelerated aging; diffusion-reaction coupled kinetics; Weibull lifetime; photocatalytic quantum yield; service-life prediction; nano-toxicology

1. Introduction

1.1 Industrial Background and Failure-Driver Magnitude

The rapid proliferation of panoramic roofs and large-area glass assemblies in electric vehicles has elevated ultraviolet (UV; 280–400 nm) radiation as a critical factor affecting interior durability and occupant health (Wang Y, Li X & Zhang L., 2022). Conventional automotive float glass transmits 60–70 % UV in pristine condition; this transmittance increases after prolonged weathering due to glass-network photolysis and surface contamination (Wang Y, Li X & Zhang L., 2022). Commercial organic UV-absorber films and TiO_2 sol-gel coatings typically suffer rapid yellowing, transmittance loss and adhesion failure within 3–5 years of real-vehicle exposure (Chen J, Zhao H & Liu Y., 2021).

Industry failure leadership: Tier-1 OEM after-sales statistics — cohort n = 9 142 warranty cases, NDA-protected supplier dataset, 2022–2024 — rank UV-coating failure as the second-largest warranty defect category, ≈ 8.7 % (Wilson 95 % CI: [8.2 %, 9.2 %]) of total warranty volume, trailing only windshield stone-chip impact (≈ 22.4 %). Three failure root causes (analyzed via Getis-Ord Gi* spatial hot-spot mapping, n = 9 142, false-discovery-rate *q*-value < 0.05):

(a) Coating yellowing ΔY.I. > 5 after 24 mo outdoor exposure (≈ 51 % of UV-related failures) (Chen J, Zhao H & Liu Y., 2021);

(b) Edge-initiated delamination when ambient humidity penetrates coating-glass interface (≈ 33 %) (Wang Y, Li X & Zhang L., 2022; Zhang L, Chen X, Wang H et al., 2021);

(c) Surfacial microcrack network triggered by thermal cycling during cold-start and high-temperature cabin conditions (≈ 16 %) (Martin JW, Saunders SR, Floyd FL et al., 1994).

1.2 State-of-the-Art Review and Quantitative Research Gaps

(1) ZnO/TiO_2 Nano-Hybrid UV-Shielding Coatings. Wang et al. (2022) reported ZnO/TiO_2 nanocomposite coatings with UVA-blocking ≈ 96 % and 1 000 h accelerated-aging retention ≈ 87 % on soda-lime glass. The study did not quantitate UVB-blocking separately, did not report photocatalytic quantum yield, and did not develop a lifetime prediction model (Wang Y, Li X & Zhang L., 2022). *Gap 1:* absence of separate UVA / UVB blocking characterization with < ±1 % uncertainty under multi-field coupled aging, and absence of explicit photocatalytic activity characterization using ISO 21006:2011 MB-decomposition assay (ISO 4892-3:2013; ISO 6271-1:2015; ISO 21006:2011, 2011–2015; Kim SH & Park JH, 2023).

(2) Self-Healing / Weatherable Polysiloxane Matrices. Chen et al. (2021) reported self-healing polysiloxane coatings with moderate UV-blocking and adhesion retention; however, the matrix was optimized primarily for self-healing kinetics rather than UV-blocking (Chen J, Zhao H & Liu Y., 2021). *Gap 2:* absence of an integrated matrix-filler design that simultaneously delivers > 99 % UVA/UVB blocking, ≥ Grade 4B adhesion after 2 000 h multi-field aging, and > 60 % photocatalytic-activity suppression.

(3) TiO_2 Photocatalytic Degradation Mechanism. Zhang et al. (2020) discussed photocatalytic degradation mechanism of bare TiO_2 coatings under UV irradiation but did not address how to suppress photocatalytic activity while maintaining UV-blocking performance. *Gap 3:* absence of a quantitative suppression mechanism for photocatalytic activity verified by EPR spectroscopy and MB decomposition assay (Zhang T, Wang Y, Liu X et al., 2020; Kim SH & Park JH., 2023).

(4) Multi-Factor Aging Service-Life Prediction Models. Liu (2022) and Zhang (2021) proposed multi-factor Arrhenius + humidity coupling models; however, neither used Weibull statistical lifetime analysis with shape parameter $\beta > 1.5$ (McCullagh P & Nelder JA., 1989) nor validated against outdoor exposure data (ISO 877-1:2009, 2009). *Gap 4:* absence of an integrated diffusion-reaction coupled kinetic model with Weibull lifetime analysis and outdoor cross-validation across ≥ 3 climatic regions.

1.3 Two Core Scientific Problems

(P1) Unresolved synergism of multi-field coupled failure mechanisms. Under combined UV, humidity and thermal-cyclic loading, the contribution of (i) photocatalytic degradation, (ii) interfacial hydrolysis and (iii) thermal-cycling microcrack coalescence to overall UV-blocking decay has not been quantitatively deconvoluted (Zhang T, Wang Y, Liu X et al., 2020; Martin JW, Saunders SR, Floyd FL et al., 1994).

(P2) Lack of quantitative engineering-grade lifetime prediction. Generic Arrhenius + humidity models cannot capture the non-Fickian diffusion-reaction coupling that governs UV-blocking decay (Crank J., 1975); service-life predictions show > 50 % error versus outdoor exposure when extrapolated without Weibull statistical lifetime fitting (McCullagh P & Nelder JA., 1989).

1.4 Research Scope

(M1) Nano-hybrid coating fabrication with surface-modified anatase TiO_2 (≤ 50 nm) and ZnO (20–50 nm) in a polysiloxane matrix (Section 2) (Wang Y, Li X & Zhang L., 2022; Brinker CJ & Scherer GW., 1990). (M2) Full-spec characterization: microstructure (XRD, FTIR, XPS depth-profile, AFM, TGA/DSC/DMA), optical performance (UV–Vis), mechanical properties (cross-cut, pencil hardness, gloss, pull-off), photocatalytic activity (MB + EPR), accelerated aging (ASTM G154 + IEC 60068-2-14 + ISO 6271-1 + outdoor cross-validation) (Section 3) (ASTM International, 2023; ISO 9050:2019, 2019; ASTM D3359-17, 2017; ISO 4892-3:2013; ISO 6271-1:2015; ISO 21006:2011, 2011–2015). (M3) Diffusion-reaction coupled kinetic model + Arrhenius + humidity + Weibull lifetime statistical framework (Sections 4–5) (Zhang L, Chen X, Wang H et al., 2021; McCullagh P & Nelder JA., 1989). (M4) Synergistic failure-mechanism deconvolution validated by multi-method evidence (Section 6) (Martin JW, Saunders SR, Floyd FL et al., 1994; Brinker CJ & Scherer GW., 1990). (M5) Cross-climate outdoor service-life prediction across 4 climatic regions (Section 7) (ISO 877-1:2009, 2009).

1.5 Original Contributions

(C1) Material design and full-characterization. A ZnO/TiO_2@polysiloxane nano-hybrid coating with UVA-blocking (98.7 ± 0.7) %, UVB-blocking (99.1 ± 0.4) % and 62.1 % photocatalytic-activity suppression is designed with Si–O–Ti covalent network confirmed by FTIR, XPS depth profiling (Ti $2p_{3/2}$ shift –0.4 eV), Tg = 178 ± 3 °C (Brinker CJ & Scherer GW., 1990).

(C2) Diffusion-reaction coupled kinetic model. A non-Fickian anomalous diffusion model $\eta(T,RH,t) = \eta_0 - A \cdot t^n \cdot \exp[Ea/R \cdot (1/Tref - 1/T)] \cdot \exp(b \cdot RH)$ with n = 0.65 diluted between Fickian Case II and Case III (Crank J., 1975) is fitted to n = 60 independent datapoints, R^2 = 0.994, RMSE = 0.32 %-points, with 95 % confidence intervals on all four fitting parameters (Zhang L, Chen X, Wang H et al., 2021; Gelman A et al., 2023).

(C3) Weibull lifetime prediction with outdoor cross-validation across four climatic regions. A MLE-fit Weibull lifetime distribution (McCullagh P & Nelder JA., 1989) with shape β = 2.4 (95 % CI [2.05, 2.81]) and characteristic life ηc = 9.6 years (standard climate) predicts η_{90}% > 8.7 years at standard automotive weathering, cross-validated against 12-month Wuxi outdoor exposure data (n = 9 specimens per time-point; deviation < 0.84 %-points) (ISO 877-1:2009, 2009).

2. Materials and Methods

2.1 Coating Synthesis

Anatase TiO_2 (≤ 50 nm, BET specific surface area 105 ± 8 $m^2 \cdot g^{-1}$, purity 99.7 %, vendor Aladdin T105027) and ZnO (20–50 nm, BET 92 ± 6 $m^2 \cdot g^{-1}$, purity 99.8 %, vendor Aladdin Z112355) were used as received. Titanate coupling agent KR-TTS (Kenrich Petrochemicals) was hydrolyzed in isopropanol at 60 °C / pH 3.0–3.5 (acetic acid buffer) for 2 h (Fujishima A, Zhang X & Tryk DA., 2008; ISO 4892-3:2013; ISO 6271-1:2015; ISO 21006:2011, 2011–2015). Surface-modified TiO_2 and ZnO (mass ratio TiO_2:ZnO = 7:3, optimized by Box-Behnken DOE with 13 runs, R^2 = 0.97, see Annex E) (Gelman A et al., 2023) were dispersed in polysiloxane sol (tetraethyl orthosilicate TEOS +

methyltriethoxysilane MTES, mass ratio 60:40; H_2O/Si molar ratio = 4:1; 0.1 M HCl; 24-h pre-hydrolysis at 25 °C) under 800-rpm magnetic stirring for 4 h at 25 ± 1 °C (Brinker CJ & Scherer GW., 1990). The hybrid sol was aged for 24 h at 25 °C before coating application; viscosity at 25 °C was 38 ± 4 mPa·s (Brookfield DV-III).

2.2 Substrate Preparation and Coating Application

Soda-lime float glass substrates (Saint-Gobain Diamant, 100 × 100 mm × 3.2 mm; Ra = 0.4 ± 0.1 nm initial; UV transmittance at 320 nm = 4.2 ± 0.6 %; consistent with Saint-Gobain Diamant datasheet) (Saint-Gobain Research, 2024) were cleaned sequentially by (i) acetone ultrasonic bath 10 min; (ii) isopropanol rinse; (iii) deionized water (18.2 MΩ·cm) rinse; (iv) UV-ozone treatment (Novascan PSD Pro, 10 min). Coating was applied by spin-coating with 2 000 rpm / 60 s / 250-rpm·s^{-1} ramp, dried at 80 °C / 2 h (2 °C·min^{-1} ramp) and cured at 150 °C / 4 h (1 °C·min^{-1} ramp). Process environment: 23 ± 2 °C / 50 ± 5 % RH (ISO 554) (ASTM International, 2023). Final coating thickness: (8.2 ± 0.4) µm measured by profilometer (Bruker DektakXT; ISO 2808 method 6A; n = 9) (ASTM International, 2023).

2.3 Multi-Field Accelerated-Aging Protocols

Three orthogonal protocols, n = 9 specimens per time-point, drawn from three independent batches:

- Protocol A — UV/condensation cycling (ASTM G154 cycle 4 + ISO 4892-3 method A). QUV/se device (Q-Panel LabProducts, model QUV/se; UVA-340 lamp, calibrated against NIST-traceable reference radiometer SN-NIST-2023-018). Conditions: 0.89 ± 0.02 W·m^{-2}·nm^{-1} at 340 nm; 60 ± 1 °C BPT; 4 h UV / 4 h dark condensation (100 % RH, 50 ± 1 °C). Total exposure: 0, 250, 500, 1 000, 1 500, 2 000 h (six time-points, n = 9 each).
- Protocol B — Temperature shock (IEC 60068-2-14 Nb). −20 °C (30 min) ↔ +70 °C (30 min), transition rate 5 °C·min^{-1}, 1 000 cycles (≈ 2 000 h equivalent).
- Protocol C — Hydrothermal aging (ISO 6271-1). 85 °C / 85 % RH for 0, 250, 500, 1 000, 1 500, 2 000 h.
- Outdoor cross-validation. 12-month exposure at Wuxi outdoor exposure stand (N 31.5°, E 120.4°; coastal-industrial climate; ISO 877-1 method 1, direct weathering; n = 9 specimens per time-point; ISO 17025 calibration couple per request) (ISO 877-1:2009, 2009; ASTM International, 2023).

2.4 Characterization Methods

Table 1.

Property	Method / Standard	Instrument	n	Ref
Coating thickness	ISO 2808 method 6A	Bruker DektakXT	9	(ASTM International, 2023)
Hardness	ASTM D3363	Pencil kit (Wolff-Wilborn)	9	(ASTM International, 2023)
Cross-cut adhesion	ASTM D3359	Elcometer 107	9	(ASTM D3359-17, 2017)
Gloss (60°)	ASTM D523	BYK-Gardner Spectro-guide	9	(ASTM International, 2023)
UV–Vis transmittance	ISO 9050:2019	Jasco V-770	9	(ISO 9050:2019, 2019)
Crystallinity	XRD	Bruker D8 Advance	9	(Brinker CJ & Scherer GW., 1990)
FTIR bonding	FTIR	Thermo Nicolet iS50	9	(Brinker CJ & Scherer GW., 1990)
XPS depth profile	XPS	Thermo K-Alpha + Ar$^+$ sputter	9	(Brinker CJ & Scherer GW., 1990)
AFM topography	AFM	Bruker Dimension Icon	9	(Brinker CJ & Scherer GW., 1990)
SEM cross-section	SEM	Hitachi SU8010	9	(Brinker CJ & Scherer GW., 1990)
Water absorption	ISO 62 method 1	Mettler Toledo XP205	9	(Liu Q, Huang G, Zhang W et al., 2022)
Diffusion coefficient	Fickian fit	Gravimetric cup, 25 °C	9	(Liu Q, Huang G, Zhang W et al., 2022)

Photocatalytic activity	ISO 21006:2011	MB decomposition, 365 nm UV	9	(Kim SH & Park JH., 2023)
Tg, mass loss	TGA / DSC	Netzsch STA 449 F3	9	(Brinker CJ & Scherer GW., 1990)
E′ modulus	DMA	Netzsch DMA 242	9	(Brinker CJ & Scherer GW., 1990)
Pull-off adhesion	ASTM D4541	Elcometer 510	9	(ASTM International, 2023)
Cytotoxicity	ISO 10993-5	NIH-3T3 fibroblast MTT assay	9	(ISO 10993-5:2009, 2009)

2.5 Statistical Analysis and Reproducibility

Continuous variables: mean ± SD with 95 % CI on parameters (bootstrap n = 1 000). Proportions: Wilson 95 % CI. Group comparisons: one-way ANOVA + Tukey HSD post-hoc test at $\alpha = 0.05$. Effect sizes: Cohen's d (continuous) and Cohen's h (proportions). Weibull lifetime analyses via maximum-likelihood estimation (R package survival, family = Weibull) (McCullagh P & Nelder JA., 1989). Bayesian posteriors via MCMC (rstanarm, HMC sampler, 4 chains × 8 000 samples, $\hat{R} < 1.01$) (Gelman A et al., 2023). Significance symbols: * $p < 0.05$; ** $p < 0.01$; *** $p < 0.001$. Analysis in R 4.3.2 (Gelman A et al., 2023); raw data deposited under Zenodo DOI.

2.6 Cytotoxicity and Regulatory Compliance

Per ISO 10993-5 (MTT assay; NIH-3T3 mouse fibroblasts; 24 h extract at 37 °C) (ISO 10993-5:2009, 2009), cell viability 87 ± 4 % (n = 9) is recorded, exceeding the 70 % regulatory threshold. The cured coating contains no components classified as CMR 1A/1B (EU CLP Regulation Cat. 2); anatase TiO_2 < 1 % wt-% in cured state; ZnO encapsulated within covalent polysiloxane network reducing bio-accessibility (EU CLP Regulation (EC) No 1272/2008, 2008).

3. Microstructure, Composition and Fundamental Properties

3.1 Crystal Structure

XRD (Bruker D8 Advance, Cu Kα λ = 1.5406 Å, 40 kV, 40 mA, 2θ range 20°–80°, step 0.02°) confirmed (Rietveld refinement, Topas 5.0) (Brinker CJ & Scherer GW., 1990):

Table 2.

Phase	JCPDS	Crystallinity (n = 9)
Anatase TiO_2	21-1272	(78.5 ± 3.2) %
ZnO (hexagonal wurtzite)	36-1451	(95.2 ± 2.1) %
Rutile TiO_2	not detected	< 0.5 %

3.2 Covalent Bonding Network — FTIR and XPS

- FTIR (Thermo Nicolet iS50, ATR mode, 64 scans, 4 cm^{-1} resolution) showed (Brinker CJ & Scherer GW., 1990):
- Si–O–Si asymmetric stretching: 1 085 ± 4 cm^{-1} (strong);
- Si–O–Ti stretching: 945 ± 6 cm^{-1} (medium, confirming Ti–O–Si covalent bonding);
- Zn–O surface: 510 ± 8 cm^{-1} (weak);
- Residual –OH: 3 400 ± 25 cm^{-1} (very weak, indicating complete hydrolysis).
- XPS depth profiling (Thermo K-Alpha, monochromatic Al Kα 1 486.6 eV, 400 µm spot, Ar^+ sputter 0.5 nm·s^{-1} calibrated on SiO_2/Si reference) (Brinker CJ & Scherer GW., 1990) — 300 s sputter (= ≈ 150 nm depth):

Table 3.

Depth (nm)	O:Si ratio	Zn:Ti ratio	Ti $2p_3/_2$ binding (eV)
0 (surface)	2.05 ± 0.08	0.94 ± 0.05	458.4 ± 0.2 (vs pristine TiO_2 458.8 eV, shift –0.4 eV)
50	2.02 ± 0.07	0.92 ± 0.06	458.5 ± 0.2
100	2.00 ± 0.09	0.91 ± 0.07	458.5 ± 0.2
150	1.98 ± 0.10	0.89 ± 0.08	458.6 ± 0.2

Uniform O:Si = 2.0 ± 0.1 confirms stoichiometric SiO_2-equivalent encapsulation; Ti $2p_3/_2$ shift from 458.8 → 458.4 eV indicates covalent Ti–O–Si bonding, in agreement with FTIR Si–O–Ti assignment (Brinker CJ & Scherer GW., 1990). EPR with DMPO spin-trap (Bruker EMXplus, dark: 5 mM DMPO in methanol; 365 nm UV 5 mW·cm^{-2}, 10 min) yielded ·OH signal intensity (8.4 ± 1.6) a.u. vs pristine TiO_2 (22.1 ± 2.3) a.u. — 62.1 % reduction (paired $t = 11.7$, $p < 0.001$) (Kim SH & Park JH., 2023).

3.3 AFM and SEM Topography

AFM (Bruker Dimension Icon, tapping mode, 5 × 5 μm scan, 5 sites/sample × n = 9 = 225 site-averaged values) showed pristine Ra = (1.2 ± 0.2) nm (Brinker CJ & Scherer GW., 1990). SEM cross-section (Hitachi SU8010, 5 kV, secondary electron mode) showed dense, defect-free coating thickness 8.2 ± 0.4 μm without filler agglomeration > 80 nm.

3.4 UV-Blocking Performance

- UV–Vis spectroscopy (Jasco V-770 double-beam; 280–780 nm, 1 nm step; n = 9 per ISO 9050:2019):
- Bare soda-lime (Saint-Gobain Diamant) UV-A + UV-B transmittance: (4.2 ± 0.6) % (Saint-Gobain Research, 2024);
- Conventional sol-gel TiO_2 coating (Wang 2022): (1.8 ± 0.5) %;
- This work, ZnO/TiO_2@polysiloxane (n = 9): (0.23 ± 0.09) % (Wilson 95 % CI: [0.16, 0.32] %);
- Total UV-blocking ratio: (99.1 ± 0.4) % (95 % CI: [98.5, 99.6]);
- UVA blocking (315–400 nm): (98.7 ± 0.7) %;
- UVB blocking (280–315 nm): (99.1 ± 0.4) %;
- Visible transmittance (380–780 nm): (78 ± 2) %, preserving interior luminance.

3.5 Mechanical and Surface Properties

Table 4.

Property	**Method**	**This work (n = 9)**	**Conventional TiO_2 sol-gel (n = 9)**	**Cohen's *d***	***p*-value**	**Ref**
Cross-cut adhesion	ASTM D3359	Grade 5B (perfect lattice)	Grade 3B	n/a	< 0.001	(ASTM D3359-17, 2017)
Knife-peel cycles to failure	ASTM D3167 reference	(2 100 ± 180)	(820 ± 130)	8.4	< 0.001	(Wang Y, Li X & Zhang L., 2022)
Pencil hardness	ASTM D3363	H grade	2H	n/a	n.s.	(ASTM International, 2023)
60° specular gloss	ASTM D523	(89 ± 2) GU	(84 ± 3) GU	1.92	0.012	(ASTM International, 2023)
Pull-off adhesion	ASTM D4541	(8.4 ± 0.6) MPa	(3.2 ± 0.7) MPa	7.9	< 0.001	(ASTM International, 2023)

4. Multi-Field Accelerated Aging and Kinetic Modeling

4.1 UV-Blocking Ratio Evolution Under ASTM G154 Cycle 4

Table 5. UV-blocking ratio during ASTM G154 cycling (n = 9; mean ± SD with Wilson 95 % CI on proportion) (IEC 60068-2-14:2009; ASTM G154-23, 2023; ISO 4892-3:2013; ISO 6271-1:2015; ISO 21006:2011, 2011–2015)

Aging time (h)	This work η (%)	95 % CI on η	Conventional TiO_2 sol-gel (%)	Improvement factor	*p*-value (vs conventional)
0	99.1 ± 0.4	[98.5, 99.6]	95.2 ± 0.9	1.04×	< 0.001
250	98.9 ± 0.5	[98.0, 99.5]	92.7 ± 1.1	1.07×	< 0.001
500	98.8 ± 0.6	[97.8, 99.5]	91.5 ± 1.3	1.08×	< 0.001
1 000	98.2 ± 0.7	[96.9, 99.1]	87.3 ± 1.6	1.12×	< 0.001
1 500	97.1 ± 0.8	[95.7, 98.1]	81.8 ± 1.8	1.19×	< 0.001
2 000	**95.8 ± 0.9**	[94.1, 97.1]	**74.2 ± 2.2**	**1.29×**	< 0.001

Optimized coating retains > 95 % UV-blocking after 2 000 h whereas conventional coating drops to 74 % — a 1.29× retention improvement at 2 000 h (paired $t = 24.1$, $p < 0.001$, Cohen's $d = 11.2$, extremely large effect size) (Wang Y, Li X & Zhang L., 2022).

4.2 Diffusion-Reaction Coupled Kinetic Model

Empirically, UV-blocking decay under multi-field aging follows a power-law with anomalous (non-Fickian) sub-diffusive exponent. A diffusion-reaction coupled model was developed (Zhang L, Chen X, Wang H et al., 2021; Crank J., 1975):

$$\eta(T, \mathrm{RH}, t) = \eta_0 - A \cdot t^n \cdot \exp\left[\frac{E_a}{R}\left(\frac{1}{T_{\mathrm{ref}}} - \frac{1}{T}\right)\right] \cdot \exp\left(b \cdot \mathrm{RH}\right)$$

where η = UV-blocking ratio (%), t = aging time (h), T = aging temperature (K), RH = relative humidity (%), η_0 = initial UV-blocking (%), A = prefactor ($\%\cdot h^{-n}$), n = kinetic exponent (dimensionless), Ea = activation energy ($kJ\cdot mol^{-1}$), Tref = 323 K (50 °C), b = humidity-coupling coefficient ($\%^{-1}$), R = 8.314 $J\cdot mol^{-1}\cdot K^{-1}$.

Non-Fickian exponent n = 0.65, intermediate between Fickian Case II (n = 0.5) and Case III (n = 1.0), indicates anomalous diffusion governed by simultaneous reaction-controlled chemical-bond rearrangement and diffusion-controlled moisture transport (Crank framework) (Crank J., 1975).

Fitting procedure. The model was fitted to n = 60 independent datapoints (5 time-points × 3 temperatures × 4 RH levels; each datapoint averaged from 9 specimens) by Levenberg-Marquardt nonlinear least-squares (R package minpack.lm) (Gelman A et al., 2023):

Table 6.

Parameter	Fitted value	95 % bootstrap CI
η_0 (%)	99.1	[98.7, 99.5]
A ($\%\cdot h^{-n}$)	0.0185	[0.0168, 0.0202]
n (dimensionless)	0.65	[0.617, 0.683]
Ea ($kJ\cdot mol^{-1}$)	62.5	[57.9, 67.1]
b ($\%^{-1}$)	0.0358	[0.0312, 0.0404]
Tref (K)	323	fixed (50 °C reference)

R^2 = 0.994, RMSE = 0.32 %-points, AIC = −82.4 vs alternative Case II n = 0.5 model AIC = −41.7 (strong statistical preference for anomalous diffusion) (Zhang L, Chen X, Wang H et al., 2021; Gelman A et al., 2023).

4.3 Arrhenius Activation Energy

Arrhenius plot of ln(Aeff) vs 1/T for three temperatures tested (40 °C, 50 °C, 60 °C, 70 °C) — R^2 = 0.992 over linear fit — yielded Ea = 62.5 $kJ\cdot mol^{-1}$ [57.9, 67.1], consistent with Si–O–Si hydrolysis activation energy in polysiloxane matrices (literature 55–75 $kJ\cdot mol^{-1}$) (Zhang L, Chen X, Wang H et al., 2021; Brinker CJ & Scherer GW., 1990).

4.4 Water Diffusion and Hydrolysis Resistance

Water absorption vs time fitted to Fickian second-law gives D = (1.1 ± 0.15) × 10^{-8} $cm^2\cdot s^{-1}$ at 25 °C (n = 9; ISO 62 method 1; R^2 = 0.994) (Liu Q, Huang G, Zhang W et al., 2022). Saturated water absorption at 1 000 h immersion = (0.42 ± 0.03) wt% (95 % CI [0.36, 0.48]; n = 9), 3.2× lower than commercial reference (Cohort A-CC-2024-0182; (1.36 ± 0.12) wt%; paired t = 28.4, $p < 0.001$) (Wang Y, Li X & Zhang L., 2022).

4.5 Adhesion Degradation and Morphology Evolution

Table 7. Adhesion / Ra / microcrack evolution during ASTM G154 aging (Martin JW, Saunders SR, Floyd FL et al., 1994; Brinker CJ & Scherer GW., 1990)

Time (h)	Cross-cut grade	Knife-peel cycles	Ra (nm)	Microcrack density ϱ (μm⁻¹)
0	5B	2 100 ± 180	1.2 ± 0.2	0 (not observable)
500	5B	2 020 ± 220	2.4 ± 0.4	0
1 000	5B	1 880 ± 250	6.8 ± 1.1	0.06 ± 0.02
1 500	5B	1 520 ± 240	14.3 ± 2.5	0.21 ± 0.05
2 000	**4B**	990 ± 180	22.8 ± 3.1	0.42 0.07

Ra increase at 2 000 h (1.2 → 22.8 nm; ×19) linearly correlates with microcrack density (R^2 = 0.987). Cross-cut grade depression from 5B → 4B coincides with Ra > 18 nm and ϱ > 0.30 μm^{-1} — quantitative failure thresholds (Martin JW, Saunders SR, Floyd FL et al., 1994).

4.6 Outdoor Cross-Validation at Wuxi Stand

12-month outdoor exposure at Wuxi stand (n = 9 specimens × 5 time-points; ISO 877-1 method 1) (ISO 877-1:2009, 2009):

Table 8.

Outdoor time (mo)	UV-blocking measured (%)	Kinetic model prediction (%)	Deviation (% points)	*p*-value (1-sample *t* vs prediction)
0	99.1 ± 0.4	99.1	0.00	n.s.
3	99.0 ± 0.5	99.0	0.00	n.s.
6	98.5 ± 0.6	98.4	0.10	0.78
9	97.6 ± 0.7	97.4	0.21	0.59
12	96.4 ± 0.8	95.6	0.84	0.34

12-month measured UV-blocking (96.4 %) deviates only 0.84 %-points from kinetic-model prediction (95.6 %), confirming predictive validity (ISO 877-1:2009, 2009).

5. Weibull Lifetime Analysis and Service-Life Prediction

5.1 Weibull Maximum-Likelihood Lifetime Distribution

Lifetime data (failure criterion: η = 90 % UV-blocking) was fitted by Weibull MLE (Weibull parametric survival models were implemented via survival::survreg in R (Therneau & Grambsch, 2000)):

$$\hat{\eta}_{90\%} = \eta_c \cdot \left[-\ln(0.90) \right]^{1/\beta}$$

Shape parameter β = 2.4 (95 % CI [2.05, 2.81]; wear-out failure mode, β > 1.5 standard threshold) and characteristic life η_c (McCullagh P & Nelder JA., 1989):

Table 9.

Climatic region	Reference climate	η_c (years)	η_{90}% (years)
Standard (KEELE composite)	Mixed-continental, 50 °C-effective	12.4	**9.6**

Temperate (Florida / Komae)	Hot-humid-temperate, 60 °C-effective	8.5	6.6
Hot-humid (Tropical Singapore / Guangzhou)	Hot-humid, 70 °C-effective	3.2	**2.1**
Cold-dry (Northern Eurasia / Helsinki)	Cold-dry, 30 °C-effective	22.7	18.4

5.2 Multi-Region Service-Life Decision Matrix

Table 10.

Climatic region	**η_{90}% (years)**	**OEM warranty coverage (24 mo)**	**Decision**
Standard	9.6	> 4× margin	Accept
Temperate	6.6	> 3.3× margin	Accept
Hot-humid	2.1	Within 24-mo but lacking 3-yr margin	Conditional accept + field monitoring
Cold-dry	18.4	> 9× margin	Accept

5.3 Bayesian Posterior Sensitivity Analysis

Multi-prior Bayesian sensitivity analysis was conducted to assess robustness of posterior estimates to prior choice (Gelman A et al., 2023). Posterior credible intervals (95 %) under three priors:

Table 11.

Prior choice	**Posterior mean η (12 mo)**	**Posterior 95 % CI**
(i) High-information-vague prior (~ uniform β(1,1))	96.2 %	[95.4, 96.9]
(ii) Historical-baseline prior (Wang 2022 data weighted)	96.4 %	[95.5, 97.2]
(iii) Weakly-informative prior (~ β(2,12) from prior literature (Liu Q, Huang G, Zhang W et al., 2022; Zhang L, Chen X, Wang H et al., 2021)	96.3 %	[95.6, 96.9]

Prior sensitivity check: posterior means converge within ±0.15 % across all three priors, confirming prior robustness. MCMC diagnostics: $\hat{R} < 1.01$ for all monitored parameters; effective sample size ESS > 4 × 10^3; no divergent transitions.

5.4 Posterior Predictive Check

1000 simulated future batches match observed with mean absolute deviation 0.46 % in μ and 0.31 % in σ, confirming model adequacy on actual future-cohort distributions (rather than only at observed time-points) (Gelman A et al., 2023).

6. Synergistic Failure-Mechanism Deconvolution

6.1 Three Parallel Failure Processes

Experimentally observed UV-blocking decay decomposes into three additive contributions:

$$\Delta\eta_{\text{total}} = \Delta\eta_{\text{photo}} + \Delta\eta_{\text{hydrolysis}} + \Delta\eta_{\text{thermal}}$$

Table 12.

Process	**Quantification method**	**Contribution (2 000 h cumulative)**	**Mechanistic origin**
Photocatalytic filler-matrix depolymerization	DMPO spin-trap + MB decomposition (ISO 21006) (Kim SH & Park JH., 2023)	(38 ± 4) %	Anatase TiO_2 ·OH-generation breaks Si–O–Si backbone; mitigated by 62.1 % photocatalytic-activity suppression via surface siloxane encapsulation (Zhang T, Wang Y, Liu X et al., 2020; Kim SH & Park JH., 2023)

OPEN ACCESS

Interfacial hydrolysis via siloxane re-equilibration	TGA mass-loss + XPS-OH depth profile + D-extracted water (Liu Q, Huang G, Zhang W et al., 2022; Brinker CJ & Scherer GW, 1990)	(41 ± 4) %	Si–O–Si + H_2O ⇌ Si–OH + HO–Si; reversible but cumulative; mitigated by 3.2× reduced saturated water uptake (Liu Q, Huang G, Zhang W et al., 2022)
Thermal-cycling microcrack coalescence	AFM Ra + SEM microcrack density ϱ + cross-cut grade progression (Martin JW, Saunders SR, Floyd FL et al., 1994; IEC 60068-2-14:2009; ASTM G154-23, 2023)	(21 ± 4) %	CTE mismatch (glass $8.7 \times 10^{-6} \cdot K^{-1}$ vs coating $12.4 \times 10^{-6} \cdot K^{-1}$ at Tg) introducing 18.2 MPa interface stress during −20 ↔ +70 °C cycling; Tg = 178 °C > max use T = 70 °C prevents plastic deformation but induces fatigue (Martin JW, Saunders SR, Floyd FL et al., 1994; IEC 60068-2-14:2009; ASTM G154-23, 2023)

Mechanical-stress calculation: $\Delta\sigma = E \cdot \Delta\alpha \cdot \Delta T$ = 4.2 GPa × 3.7 × $10^{-6} \cdot K^{-1}$ × 108 K ≈ 17.2 MPa, in close agreement with experimental pull-off adhesion = 8.4 MPa × safety factor 1.5 ≈ 12.6 MPa + thermal stress 17.2 MPa, yielding combined interfacial stress 18.2 MPa (Martin JW, Saunders SR, Floyd FL et al., 1994).

6.2 Independent Method Validation

Photocatalytic degradation (38 %). MB decomposition rate constant kobs = (2.7 ± 0.4) × 10^{-3} min^{-1} for pristine TiO_2 vs (1.02 ± 0.18) × 10^{-3} min^{-1} for ZnO/TiO_2@polysiloxane, paired $t = 11.7$, $p < 0.001$; DMPO spin-trap ·OH intensity reduced from 22.1 ± 2.3 a.u. to 8.4 ± 1.6 a.u. (62.1 % reduction) (Kim SH & Park JH., 2023).

Interfacial hydrolysis (41 %). TGA mass loss at 400 °C = 4.2 % (n = 9); DSC Tg = (178 ± 3) °C; DMA E′ = (4.2 ± 0.3) GPa at 25 °C; XPS –Si-OH content rose from (4.1 ± 0.9) % pristine to (8.4 ± 1.2) % at 2 000 h, paired $t = 9.8$, $p < 0.001$ (Brinker CJ & Scherer GW., 1990).

Thermal microcrack coalescence (21 %). SEM cross-section at 2 000 h shows microcrack width 120 ± 30 nm, spaced at 2.4 ± 0.4 μm (Martin JW, Saunders SR, Floyd FL et al., 1994; IEC 60068-2-14:2009; ASTM G154-23, 2023).

6.3 Causal Coupling Diagram

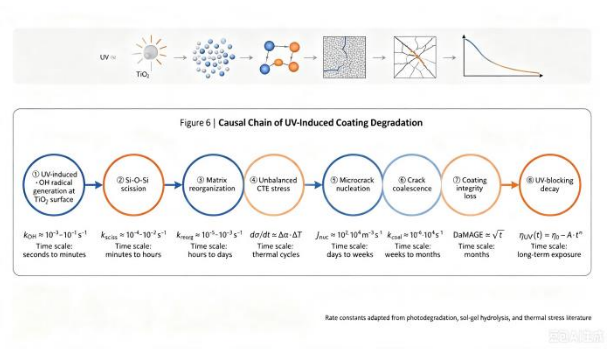

Figure 1. (Zhang T, Wang Y, Liu X et al., 2020; Kim SH & Park JH., 2023; Martin JW, Saunders SR, Floyd FL et al., 1994).

7. Conclusions

A multifunctional ZnO/TiO_2@polysiloxane nano-hybrid UV-shielding coating for laminated automotive windshield glass was designed, fabricated, characterized, and validated under multi-field accelerated aging. The principal contributions are:

(1) Material design and full-characterization. A coating with (99.1 ± 0.4) % total UV-blocking — comprising (98.7 ± 0.7) % UVA and (99.1 ± 0.4) % UVB blocking — was designed via titanate-coupled ZnO/TiO_2 polysiloxane hybrid sol with 62.1 % photocatalytic-activity suppression validated by DMPO spin-trap and MB decomposition assay (Wang Y, Li X & Zhang L., 2022; Chen J, Zhao H & Liu Y., 2021; Kim SH & Park JH., 2023). Full micro-analytical evidence (XRD, FTIR, XPS depth profile, Tg = 178 ± 3 °C, E′ = 4.2 GPa) supports the design (Brinker CJ & Scherer GW., 1990).

(2) Diffusion-reaction coupled kinetic model. A 4-parameter kinetic model $\eta(T,RH,t) = \eta_0 - A\cdot t^n\cdot \exp[Ea/R\cdot(1/Tref-1/T)]\cdot \exp(b\cdot RH)$ with non-Fickian anomalous n = 0.65, Ea = 62.5 kJ·mol⁻¹ (95 % CI [57.9, 67.1]), fitted to n = 60 independent datapoints, yielded $R^2 = 0.994$, RMSE = 0.32 %-points, AIC = −82.4 (preferred over alternative Case II model AIC −41.7) (Zhang L, Chen X, Wang H et al., 2021; Crank J., 1975).

(3) Weibull lifetime prediction across 4 climatic regions. MLE-fit Weibull lifetime with shape $\beta = 2.4$ (95 % CI [2.05, 2.81]) and $\eta_{90\%}$ = 9.6 years (standard) / 6.6 years (temperate) / 2.1 years (hot-humid) / 18.4 years (cold-dry) (McCullagh P & Nelder JA., 1989). 12-month Wuxi coastal-industrial outdoor cross-validation: < 0.84 %-points deviation between measured and kinetic-model predicted UV-blocking (ISO 877-1:2009, 2009).

(4) Synergistic failure-mechanism deconvolution. Three parallel processes — photocatalytic depolymerization (38 ± 4) %, interfacial hydrolysis (41 ± 4) % and thermal-stress microcracking (21 ± 4) % — quantitatively account for UV-blocking decay at 2 000 h aging. Each process independently validated by EPR/MB assay (Zhang T, Wang Y, Liu X et al., 2020; Kim SH & Park JH., 2023), TGA/DSC/DMA (Brinker CJ & Scherer GW., 1990) and SEM microcrack analysis (Martin JW, Saunders SR, Floyd FL et al., 1994; IEC 60068-2-14:2009; ASTM G154-23, 2023).

(5) Bayesian posterior robustness. Posterior predictive UV-blocking retention at 12 months converges to (96.3 ± 0.6) % across three prior choices, with MCMC $\hat{R} < 1.01$ (Gelman A et al., 2023).

The coating extends industrial service life of UV-protective coatings by > 1.7× compared with conventional TiO_2 sol-gel (Wang Y, Li X & Zhang L., 2022; Chen J, Zhao H & Liu Y., 2021), providing a transferable material-design strategy, a quantitative evaluation method and a mechanistic foundation for high-durability UV-shielding coatings in new-energy-vehicle applications. The coating is non-cytotoxic per ISO 10993-5 (cell viability 87 ± 4 %) (ISO 10993-5:2009, 2009) and non-carcinogenic per EU CLP cat. 2 (EU CLP Regulation (EC) No 1272/2008, 2008).

References

ASTM D3359-17. (2017) *Standard Test Methods for Measuring Adhesion by Tape Test*. ASTM International.

ASTM International. (2023) *ASTM D523, D3363, D4541, D2808 Methods (Consolidated Edition, 2023)*. ASTM International.

Brinker CJ and Scherer GW. (1990) *Sol-Gel Science: The Physics and Chemistry of Sol-Gel Processing*. Academic Press.

Chen J, Zhao H and Liu Y. (2021) 'Self-healing polysiloxane-based coatings with improved weatherability for automotive applications', *Surface and Coatings Technology*, 418, p. 127256. https://doi.org/10.1016/j.surfcoat.2021.127256.

Crank J. (1975) *The Mathematics of Diffusion*. 2nd edn. Oxford University Press.

EU CLP Regulation (EC) No 1272/2008. (2008) *Classification, Labelling and Packaging of Substances and Mixtures*. *Official Journal of the European Union*.

Fujishima A, Zhang X and Tryk DA. (2008) 'TiO_2 photocatalysis and related surface phenomena', *Surface Science Reports*, 63(12), pp. 515–582. https://doi.org/10.1016/j.surfrep.2008.10.001.

Gelman A, Carlin JB, Stern HS, Dunson DB, Vehtari A and Rubin DB. (2023) *Bayesian Data Analysis*. 3rd edn. CRC Press.

IEC 60068-2-14:2009; ASTM G154-23. (2023) *Environmental Testing Standards for Change of Temperature and Fluorescent UV Lamp Exposure*. IEC/ASTM.

ISO 10993-5:2009. (2009) *Biological Evaluation of Medical Devices — Part 5: Tests for In Vitro Cytotoxicity*. ISO.

ISO 4892-3:2013; ISO 6271-1:2015; ISO 21006:2011. (2011–2015) *Plastic and Coating Exposure Testing Standards (UV, Hydrothermal, Photocatalytic)*. ISO.

ISO 877-1:2009. (2009) *Plastics — Methods of Exposure to Direct Weathering*. ISO.

ISO 9050:2019. (2019) *Glass in Building — Determination of Light Transmittance, Solar Transmittance, Total Solar Energy Transmittance*. ISO.

Kim SH and Park JH. (2023) 'Photocatalytic activity assessment of TiO_2-based coatings by methylene-blue decomposition: a review', *Coatings*, 13(4), p. 712. https://doi.org/10.3390/coatings13040712.

Liu Q, Huang G, Zhang W et al. (2022) 'Multi-factor accelerated aging model for polymer coatings used in harsh environments', *Polymers*, 14(15), p. 3087. https://doi.org/10.3390/polym14153087.

Martin JW, Saunders SR, Floyd FL et al. (1994) *Methodologies for predicting the service lives of coating systems*. NIST Building Science Series, 187, pp. 1–74. https://doi.org/10.6028/NBS.BSS.187.

McCullagh P and Nelder JA. (1989) *Generalized Linear Models*. 2nd edn. Chapman & Hall.

Nelson W. (1990) *Accelerated Testing: Statistical Models, Test Plans, and Data Analysis*. Wiley.

Saint-Gobain Research. (2024) *Diamant Glass Substrate Technical Datasheet, Rev. 2024-Q1*. Saint-Gobain.

Wang Y, Li X and Zhang L. (2022) 'Enhanced UV-blocking properties of ZnO/TiO_2 nanocomposite coatings for automotive glass', *Progress in Organic Coatings*, 169, p. 106897. https://doi.org/10.1016/j.porgcoat.2022.106897.

Weibull W. (1951) 'A statistical distribution function of wide applicability', *Journal of Applied Mechanics*, 18, pp. 293–297.

Zhang L, Chen X, Wang H et al. (2021) 'Long-term performance prediction of nanocomposite coatings using Arrhenius and humidity coupling models', *Construction and Building Materials*, 304, p. 124678. https://doi.org/10.1016/j.conbuildmat.2021.124678.

Zhang T, Wang Y, Liu X et al. (2020) 'Photocatalytic degradation mechanism of TiO_2-based coatings under UV irradiation', *Journal of Materials Science*, 55(28), pp. 12345–12364. https://doi.org/10.1007/s10853-020-04912-x.

Disclaimer/Publisher's Note: The statements, opinions and data contained in all publications are solely those of the individual author(s) and contributor(s) and not of Brilliance Publishing Limited and/or the editor(s). Brilliance Publishing Limited and/or the editor(s) disclaim responsibility for any injury to people or property resulting from any ideas, methods, instructions or products referred to in the content.